An Initial Survey of White Dwarfs in the Sloan Digital Sky Survey

Hugh C. Harris¹, James Liebert², S. J. Kleinman³, Atsuko Nitta³, Scott F. Anderson⁴, Gillian R. Knapp⁵, Jurek Krzesinski^{3,6}, Gary Schmidt², Michael A. Strauss⁵, Dan Vanden Berk⁷, Daniel Eisenstein², Suzanne Hawley⁴, Bruce Margon⁸, Jeffrey A. Munn¹, Nicole M. Silvestri⁴, Allyn Smith⁹. Paula Szkody⁴, Matthew J. Collinge⁵, Conard C. Dahn¹, Xiaohui Fan², Patrick B. Hall^{5,10}, Donald P. Schneider¹¹, J. Brinkmann³, Scott Burles¹², James E. Gunn⁵, Gregory S. Hennessy¹³, Robert Hindsley¹⁴, Zeljko Ivezić⁵, Stephen Kent^{15,16}, Donald Q. Lamb¹⁶, Robert H. Lupton⁵, R. C. Nichol¹⁷, Jeffrey R. Pier¹, David J. Schlegel⁵, Mark SubbaRao¹⁶, Alan Uomoto¹⁸, Brian Yanny¹⁵, Donald G. York¹⁶

ABSTRACT

¹U.S. Naval Observatory, PO Box 1149, Flagstaff, AZ 86002-1149.

²Steward Observatory, University of Arizona, 933 N. Cherry Ave., Tucson, AZ 85721-0065.

³Apache Point Observatory, PO Box 59, Sunspot, NM 88349-0059.

⁴Dept. of Astronomy, University of Washington, Box 351580, Seattle, WA 98195-1580.

⁵Princeton University Observatory, Peyton Hall, Princeton, NJ 08544-1001.

⁶Obserwatorium Astronomiczne na Suhorze, Akademia Pedagogicazna w Krakowie, ulica Podchorążych 2, PL-30-084 Kraków, Poland.

⁷Dept. of Physics and Astronomy, University of Pittsburgh, 3941 O'Hara Street, Pittsburgh, PA 15260.

⁸Space Telescope Science Institute, 3700 San Martin Drive, Baltimore, MD 21218.

⁹Dept. of Physics and Astronomy, University of Wyoming, P.O. Box 3905, Laramie, WY 82071.

¹⁰Departamento de Astronomía y Astrofísica, Facultad de Física, Pontificia Universidad Católica de Chile, Casilla 306, Santiago 22, Chile.

¹¹Dept. of Astronomy and Astrophysics, The Pennsylvania State University, 525 Davey Laboratory, University Park, PA 16802.

¹²Physics Department, Massachusetts Institute of Technology, 77 Massachusetts Avenue, Cambridge, MA 02139.

¹³U.S. Naval Observatory, 3450 Massachusetts Avenue, NW, Washington, DC 20392-5420.

 $^{^{14}\}mathrm{NRL/Remote}$ Sensing Division, Code 7210, Naval Research Laboratory, 4555 Overlook Avenue, SW, Washington, DC 20375.

¹⁵Fermi National Accelerator Laboratory, P.O. Box 500, Batavia, IL 60510.

 $^{^{16}}$ Department of Astronomy and Astrophysics, The University of Chicago, 5640 South Ellis Avenue, Chicago, IL 60637

¹⁷Dept. of Physics, Carnegie Mellon University, 5000 Forbes Avenue, Pittsburgh, PA 15232.

¹⁸Dept. of Physics and Astronomy, The Johns Hopkins University, 3400 North Charles Street, Baltimore, MD 21218-2686.

An initial assessment is made of white dwarf and hot subdwarf stars observed in the Sloan Digital Sky Survey. In a small area of sky (190 square degrees), observed much like the full survey will be, 269 white dwarfs and 56 hot subdwarfs are identified spectroscopically where only 44 white dwarfs and 5 hot subdwarfs were known previously. Most are ordinary DA (hydrogen atmosphere) and DB (helium) types. In addition, in the full survey to date, a number of WDs have been found with uncommon spectral types. Among these are blue DQ stars displaying lines of atomic carbon; red DQ stars showing molecular bands of C_2 with a wide variety of strengths; DZ stars where Ca and occasionally Mg, Na, and/or Fe lines are detected; and magnetic WDs with a wide range of magnetic field strengths in DA, DB, DQ, and (probably) DZ spectral types. Photometry alone allows identification of stars hotter than 12000 K, and the density of these stars for 15 < g < 20 is found to be $\sim 2.2 \text{ deg}^{-2}$ at Galactic latitudes 29–62°. Spectra are obtained for roughly half of these hot stars. The spectra show that, for 15 < g < 17, 40% of hot stars are WDs and the fraction of WDs rises to $\sim 90\%$ at g = 20. The remainder are hot sdB and sdO stars.

Subject headings: Stars: chemically peculiar — Stars: magnetic fields — Surveys — White Dwarfs

1. Introduction

There are currently 2249 known white dwarfs (WDs) with spectroscopic confirmation in the McCook & Sion (1999) catalog. These have been found in a variety of ways, but primarily the hotter stars are found as UV-excess or blue objects in imaging surveys, while the cooler stars are found in proper motion surveys. Some fairly homogeneous surveys have been published of hotter blue stars, such as the Palomar Green survey (PG: Green, Schmidt & Liebert 1986), the Kiso survey (Darling & Wegner 1996), and the more recent Hamburg/EOS surveys (Homeier et al. 1998; Christlieb et al. 2001; Koester et al. 2001). In recent years the Luyten Half Second Catalog (LHS: Luyten 1979) has been a prime source of cooler objects. Although largely complete to magnitude and color limits over 10,000 square degrees at high Galactic latitudes, the PG found fewer than 400 hot WDs to a blue magnitude limit just fainter than B = 16. Fleming, Liebert & Green (1986) analyzed the PG sample in a first comprehensive estimate of the formation rate and luminosity function of hot WDs. Other estimates, however, have suggested a somewhat higher space density of these objects, while recent estimates of the formation rate of planetary nebulae exceed the inferred formation rate of WDs (Pottasch 1996, and references therein).

Deeper imaging surveys are necessary to sample the disk scale height for WDs adequately. Boyle (1989) found a value of 275±50 pc, based on a sample of 41 stars to a magnitude limit of B=20.9. Much larger imaging surveys to fainter magnitudes than PG have been underway for several years, but only limited samples with spectroscopic confirmations have been published so

far. Like the PG, the point sources in these surveys are measured with only coarse photographic magnitudes or grism spectra and cover only a few color bands.

The Sloan Digital Sky Survey (SDSS: York et al. 2000) is obtaining deep CCD images of $10,000~\rm deg^2$ of the north Galactic cap, overlapping most of the PG but going much deeper, and in five photometric bands. The SDSS bands (u, g, r, i, and z) cover the entire optical range from the UV atmospheric cutoff (3200Å) to the detector's red sensitivity cutoff ($\sim 10,000$ Å) — see Fukugita et al. (1996) for details of the photometric system.

It was apparent from the detailed simulations of Fan (1999) that the SDSS would be very efficient in finding WDs, especially the hot objects detectable by UV-excess. This study suggested that something like 30,000 WDs would be detected to r < 19.5. Fan (1999) showed that hot WDs would be separable for the most part from quasars, compact emission-line galaxies, and other stars using their locations in the SDSS three-color (ugri) diagram. However, the WDs cooler than about 12,000 K generally would blend in with the colors of QSOs, and cooler than about 7000 K would blend with main-sequence stars. We note, however, that cool WDs with unusual spectra — energy distributions blanketed by unusually strong absorption lines or bands — could be expected to be found at different locations in the three-color diagram (Fig. 17 of Fan 1999).

In this paper we report on the WDs and other hot stars found in one region of sky (190 deg², referred to below as the 41-plate sample), as well as some WDs of special interest found elsewhere. While this sampling is in no way complete, it is shown that the basic hot DA (hydrogen atmosphere) and non-DA (helium atmosphere) sequences are identifiable, that they are found in about the numbers predicted by the Fan (1999) simulations, and that rare kinds of cooler WDs are detected as well. In Section 2 we discuss in more detail the color selection. Spectra of several different types are presented in Section 3. The final section assesses what we have learned about the potential of the SDSS from this first examination of WD candidates.

2. Color selection

The colors of WDs and other objects in the SDSS photometric system have been predicted (Fan 1999; Lenz et al. 1998) by synthesizing their colors from model atmospheres and from observed spectra. Further information is available from observed colors (Krisciunus et al. 1998; Finlator et al. 2000). A conclusion from these studies is that the hot end of the WD sequence has colors separated in SDSS color space from almost all other objects except hot subdwarfs. At temperatures cooler than about 12000 K, the WD sequence begins overlapping the colors of low-redshift QSOs and emission-line galaxies.

Objects are selected for SDSS spectroscopic observation according to numerous criteria based on each object's color and image morphology. High priority is given to QSO candidates chosen with colors outside the stellar locus (Richards et al. 2002), some of which turn out to be WDs. A small fraction of fibers remaining after galaxy, QSO, and calibration selections have been made are

assigned to candidates for different types of stars. Present categories include (1) horizontal-branch stars, (2) very cool stars, (3) cool subdwarfs, (4) carbon stars, (5) WDs with unusual colors, (6) cataclysmic variables, and (7) other objects with unusual colors. Stars in the last three categories, plus some hot stars chosen for calibration, often prove to be WDs, and are the subject of this paper.

Sky coverage in the early SDSS imaging data (Gunn et al. 1998) included most of a stripe with -1.25° < Dec < 1.25° and outside of the Galactic plane. Early spectra have been taken covering parts of this stripe. The present paper examines a sample of stars in the region with $9^{h}40 < \text{RA} < 16^{h}40$ at Galactic latitudes $29^{\circ} - 62^{\circ}$, imaged in March 1999. The spectra from 41 spectroscopic plates¹⁹ have been searched for WDs and hot subdwarfs, including most of this section of the equatorial stripe (but with a few gaps) and covering 190 deg² of sky. This sample is referred to in this paper as the 41-plate sample. A total of 264 WDs and 57 hot subdwarfs have been identified spectroscopically in this region. In addition, a number of unusual WDs found outside this region are also described here. These 41 plates also include six cataclysmic variables identified by Szkody et al. (2002) and not discussed further in this paper, as well as 18 objects with DA+M composite spectra identified by Raymond et al. (2003) and included in the following tables and figures.

Figure 1 presents SDSS color-color diagrams of the region occupied by hot stars. The classifications from the SDSS spectra of the hot WDs and subdwarfs are indicated in the diagram. In addition, the colors and magnitudes of all point sources with 15 < r < 20 in a smaller region of sky are shown. The two curves show the colors of WD model atmospheres (Bergeron et al. (1995)) with log g = 7, 8, and 9, kindly calculated and made available to us by Bergeron. The colors of all objects have been dereddened by the full reddening estimated for each line of sight (Schlegel et al. 1998), although this procedure slightly overcorrects for reddening for nearby (brighter and cooler) WDs in this sample.

Fig. 1(a) is equivalent to the well-known diagrams for WDs using UBV and uby filters (e.g. Eggen & Greenstein 1965; Graham 1972; Wegner 1979), although rotated by 90 degrees here. The sequence of WDs and hot subdwarfs with different temperatures is visible, and its separation at the hot end from most contaminating stars and QSOs is clear. In particular, WDs hotter than 12000 K are essentially uncontaminated by everything except hot subdwarfs. Horizontal branch and blue straggler stars are well-separated from all WDs by having u - g > 0.8. The scatter of WDs away from the central locus near the log g = 8 curve is larger here than has been seen in earlier studies. Probably the scatter seen here has significant contributions from random photometric errors for faint stars, from errors in the photometric calibrations, and from overcorrection for interstellar reddening for some stars (see next paragraph). The scatter of WDs in Fig. 1 is under study, pending improved reprocessing of SDSS photometry this year.

 $^{^{19}}$ These are Plates 266–269, 279–285, 291–293, 295–315, 342–346, and 348. Most are in the SDSS Early Data Release (EDR) described by Stoughton et al. 2002.

Data for the WDs and hot subdwarfs identified spectroscopically are given in Tables 1–3: DA and DB WDs in Table 1, WDs with less common spectral types in Table 2, and hot subdwarfs in Table 3. Positions at the epoch of observation (March 1999) are those from the SDSS Astrometric Pipeline (Pier et al. 2003). Magnitudes and colors are those from version 5.3 of the Photometric Pipeline (Lupton et al. 2003, in preparation) prepared for the initial Data Release 1. (Data are being reprocessed with version 5.4 of PHOTO, and ultimately will give slightly different results.) The photometric calibration is based on the SDSS standard-star system (Smith et al. 2002) tied to the Survey data with the Photometric Telescope (Hogg et al. 2001). The full interstellar absorption A_u from Schlegel et al. (1998) is given for that line of sight. Typically, the hotter stars will be at distances of several hundred pc, and they will have approximately the listed absorption at these high galactic latitudes. However, only some fraction of that absorption will apply to nearby (bright, cooler) WDs. Reddening can be calculated using E(u-g) = 0.264A(u), E(g-r) = 0.202A(u), E(r-i) = 0.129A(u), and E(i-z) = 0.119A(u); for most stars at thesehigh latitudes, the reddening is small whether or not the full absorption is correct. Proper motions are calculated using the USNO-A2.0 Catalog (Monet et al. 1999) for the first epoch position. For a few stars not in the USNO-A Catalog, usually because they are too faint to be detected on both the POSS-I blue and red plates, the first epoch position is taken from the USNO-B1.0 Catalog (Monet et al. 2003). The proper motions typically have errors of 6-8 mas yr⁻¹ rms. Where the motion is less than 20 mas yr⁻¹, it may not be real, and the position angle of the motion is omitted. Spectral types are from our classification of the SDSS spectra, as discussed in the following section.

3. White Dwarf Types

The spectra described in this section are taken with the two SDSS 2.5 m-telescope fiber spectrographs²⁰. Using fibers with a diameter of 3 arcsec, about 600 objects are observed each exposure with a resolution of about 1800. Exposures are typically 1 hr (four integrations of 15 min), depending on observing conditions to reach a target signal/noise. The spectra are extracted and calibrated automatically. Night-sky lines are not subtracted perfectly, and residuals are often seen at 5577, 5890/5896, and 6300 Åand at the near-IR end. The wavelength calibration (to heliocentric, vacuum wavelengths) is done. On rare occasions, a spurious jump remains in a spectrum at 5900 Å, where data from the blue and red detectors are combined. Spectra are corrected for terrestrial extinction, they are flux calibrated using spectrophotometric standards on each plate, and finally, they are corrected for the interstellar absorption listed in Tables 1–3.

 $^{^{20}\}mathrm{See}$ http://www.astro.princeton.edu/BBOOK/SPECTRO/spectro.html for a more complete description of this instrument.

3.1. DA, DB and DO Stars

For this preliminary analysis, spectral types are assigned on the Sion et al. (1983) system by comparison with the spectrophotometric atlas of Wesemael et al. (1993). For DA stars that appear to fall in the region (10–20,000 K) where DA Balmer line strengths are maximum, the u-g and g-r colors are also taken into account in assigning a classification. Figure 2 shows representative spectra of DA4 stars covering a range of magnitudes. In this and following figures, spectra are given in units of f_{ν} , with the peak flux density normalized to one, and with each spectrum shifted by one unit. (The coordinates and plate–fiber number are shown at the right below each spectrum.) We believe that these spectra are generally accurate enough for WD/subdwarf discrimination, and for WD classification to ± 1 subtype, for stars with g < 19.5. For the fainter stars the estimates are generally listed with a colon.

Figure 3 shows the sequence of DA types found in SDSS spectra. The sequence covers the range from DA1 to DA7, where the index is the conventional number corresponding to $50,400/T_{\rm eff}$. The sequence extends to temperatures as cool as about 7000 K, whereupon the WD colors begin blending with colors of main-sequence stars so badly that WDs are no longer selected for obtaining spectra. More accurate temperature and surface gravity determinations require fitting of the Balmer line profiles (e.g. Bergeron, Saffer & Liebert 1992); this kind of fitting has begun (Raymond et al. 2003; Nitta et al. 2003), but a discussion is deferred until a larger and more complete sample is assembled.

The majority of the DA stars appear to have $T_{\rm eff} < 25,000$ K, with very few stars showing lines weak enough or colors blue enough to be hotter than 40,000 K. Conversely, few stars have been identified at $T_{\rm eff} < 10,000$ K, a result of the color ranges chosen to identify QSO candidates for spectroscopic observation. The paucity of hotter stars is at least partly a consequence of the high Galactic latitude surveyed. It is expected that these WDs are primarily of the disk population, but the hotter WDs fainter than ~ 17 mag must lie beyond the scale height of the disk.

Examples of spectra of non-DA stars are shown in Figure 4. The non-DA stars from the 41-plate sample in Table 1 include only one hot DO star, the top spectrum in Fig. 4 (=HE1314+0018; Christlieb et al. 2001). Another cooler DO star is shown (the second spectrum) and listed in Table 2. See Dreizler & Werner (1996) for a discussion of this type of star. The few hot non-DA stars found here are consistent with the temperature distribution of DAs, although three hot DQ stars are discussed below. The third and fourth spectra show DB2 stars. The DB gap, a temperature range 30000–45000 K with no known DB stars, lies between the DO and DB2 stars. Fitting the line profiles of the second, third, and fourth spectra in Fig. 4 (and other similar stars being found by SDSS) will determine if any of these stars encroach on the DB gap. However, most DB stars in this sample appear to be confined to $T_{\rm eff} < 18,000$ K, as they do not show particularly strong He I lines characteristic of the hotter stars. The line strengths are quite sensitive to temperature over this range. The relative weakness of the 4388Å line and absence of He II 4686Å distinguishes them from helium-rich subdwarfs. He I lines are no longer visible at

this resolution at $T_{\rm eff}$ below about 12,000 K.

3.2. Magnetic White Dwarfs

A first list of magnetic WDs in the SDSS was given by Gänsicke et al. (2002) based on the EDR. Table 2 expands that list by including 22 magnetic WDs, including some spectra obtained since the EDR. Additional candidates have been found and will be discussed in a separate paper (Schmidt et al., 2003). Table 2 includes eight stars discussed by Gänsicke et al.; the stars SDSSJ1222+0015 and SDSSJ2323-0046 are omitted here, however, pending confirmation of their magnetic nature and H/He type. Figures 5 and 6 show spectra of some of the magnetic DA and DB stars, respectively. The hydrogen stars are ordered top to bottom by increasing mean field strength as indicated by the degree of Zeeman splitting. The strength of the mean surface field observed in Fig. 5 ranges from about 1 MG for the top two spectra to about 20 MG for the tenth spectrum to roughly 120 MG and 300 MG for the last two spectra. The last spectrum (SDSSJ2247+1456) has features (particularly near 5800, 7000, and 8400Å) similar to those in Grw +70°8247, a WD with a field about 320 MG (Wickramssinghe & Ferrario 1988). Detailed modelling of the line profiles is necessary in order to determine the polar field strength, the viewed inclination angle, and the degree to which the indicated field geometry is that of a centered dipole. Time-resolved spectrophotometry and/or spectropolarimetry can show whether the object is rotating.

The first and second spectra of Figure 6 are two of the simplest, low field He I spectra of magnetic WDs yet to be obtained. The Zeeman triplets of He I at 4471, 4921, 5015, 5875, and 6678Å can be matched with component positions from Kemic (1974) for a mean surface field strength of 1.9 MG for SDSSJ0142+1315 and 4.4 MG for SDSSJ0017+0041. Neither star shows any evidence for hydrogen. The third spectrum (SDSSJ0333+0007) is SDSS's recovery of the known WD HE 0330-0002 (Reimers et al. 1998; Schmidt et al. 2001). The latter authors demonstrated that the spectrum is circularly polarized, thus confirming the suggestion by the former authors that it is a magnetic WD. However, the overall energy distribution suggests a somewhat lower $T_{\rm eff}$ of 6,000-7,000 K. Thus, while there is apparent near-coincidence with some He I features, the star is too cool for significant excitation of the required lower levels. Hence, the absorption features remain of unknown origin, but are likely due to trace elements in a He-rich atmosphere.

Additional likely magnetic WDs with carbon and heavy element features, respectively, are discussed in Sections 3.3 and 3.4 below.

3.3. DQ and Peculiar DQ "Carbon" White Dwarfs

The majority of cool WDs are blackbody-like, showing weak or no spectral features, and are difficult to identify because they blend in with the normal stellar locus in two-color diagrams. Exceptions include WDs showing strong trace abundances of carbon, believed to be dredged-up from the underlying core (Wegner & Yackovich 1984; Pelletier et al. 1986). Note that stellar evolutionary models of asymptotic giant branch and pre-WDs indicate that the outer part of the carbon-oxygen core should be essentially devoid of oxygen, so that we would expect only carbon to be dredged up via its upward-diffusing tail (Salaris et al. 1997). Collectively, the WDs showing atomic and/or molecular carbon features have been classified "DQ."

Warmer DQ WDs at 12000–14000 K exhibit C I and even C II lines (see, for example, the review of WD spectra by Wesemael et al. 1993). Near 10,000 K the stars with highest C/He abundance show both atomic C I lines and C_2 "Swan" bands in their optical spectra. Lower temperature stars show only the molecular features, with five principal bandheads at 4383, 4737, 5165, 5636, and 6191Å, corresponding to the (2,0), (1,0), (0,0), (0,1), and (0,2) transitions, respectively. Each band has a sharp red edge to the absorption, degrading gradually to shorter wavelengths. Until recently, these stars have been found to temperatures as low as about 6,300 K (Bergeron, Leggett, & Ruiz 2001). Because of the low continuous opacity exhibited by neutral helium (primarily He⁻), only a little carbon is required to be detected in WDs with He-dominated atmospheres. A C/He abundance ratio of order 10^{-2} can produce C_2 bands for stars with $T_{\rm eff} \sim 10,000$ K, and the required abundance decreases with decreasing temperature, so that a ratio of 10^{-3} may suffice at 6,000 K. This opacity acts to depress the SDSS g flux (and, to a lesser extent, the r flux), thus reddening the g-r color. It also acts to redden the B-V color (Schmidt et al. 1999), and can have a dramatic effect on broadband colors.

Figure 7 shows the sequence for DQ stars with relatively weak carbon features. The spectra are arranged in order of u-i, a color that offers both a wide wavelength baseline and two bands relatively unaffected by carbon absorption, so that this ordering might approximate that by (decreasing) $T_{\rm eff}$. The top three stars in Fig. 7 show only atomic CI features; the top star is the known DQAB star WD1728+560 (G227-5). The detected CI lines are marked at the top of the figure. The fourth star (SDSSJ1148-0126) shows both CI and molecular C_2 bands, and the spectrum is nearly identical to the well-known WD0856+331 (G47-18). The remaining stars show only weak C_2 bands. Their u-i colors range from 0.0 to 0.9. Comparison with the colors of pure-He models of Bergeron et al. (1995) suggests that these stars have $T_{\rm eff} \sim 9500-6600$ K. (We emphasize, however, that the use of pure-He models to fit the slopes of the energy distributions is not likely to be accurate, since important opacities are missing. Comparison of the models with observed colors may help us define at least a relative $T_{\rm eff}$ scale.)

Figure 8 shows another sequence of stars with relatively strong C_2 Swan bands. Again, they are arranged in order of u - i color, covering a range 0.1–1.6. With three exceptions (the third, fifth, and seventh stars) the bands look fairly normal. Their colors overlap with the weak-band

stars in Fig. 7: over the range of 0.2–0.9 in u-i, corresponding to temperatures ~ 8600 –6600 K, stars are found with both weak and strong bands indicating a range of C/He abundances. The colors of the last two stars are noticeably redder than the others, and are redder than other normal DQ stars known until recently. They imply temperatures of 5500–6000 K, although pure-He models cannot be relied upon to give an accurate estimate. The ninth star (SDSSJ0935+0024) has a spectrum nearly identical to GSC2U J131147.2+292348 (Carollo et al. 2002; Carollo et al. 2003), including two of the ultraviolet band sequence of C_2 at 3852 and 4102Å; Carollo et al. (2003) derive a temperature of 5120 K for that star. The eighth star (SDSSJ0808+4640) has somewhat weaker Swan bands, but with more rounded bandheads, and does not show the ultraviolet sequence of bands. However, despite their cool temperatures, none of these two SDSS stars nor the GSC2 star appear to be the "peculiar" DQ stars discussed next.

The fifth star (SDSSJ2232-0744) in Fig. 8 appears somewhat different in having bands that are more rounded and displaced toward the blue. It may be a hybrid between the normal DQ stars and the class called "peculiar DQ" out of considerable ignorance. The latter begin appearing at temperatures below about 6300 K, with rounded, nearly symmetrical absorption bands centered at wavelengths near 4280, 4575, 5000, 5400, and 5900Å (Schmidt, Bergeron and Fegley 1995; Schmidt et al. 1999). The former authors argue that these analogous but apparently displaced bands (relative to those of C_2) are likely due to a different but related molecule. A detailed chemical equilibrium analysis of H/He/C mixtures under the physical conditions encountered in the atmospheres of these peculiar objects suggests that C_2H is a molecule preferentially formed — provided a trace abundance of hydrogen is present. To be sure, no calculations or measurements exist for molecular transitions of the C_2H molecule. The properties of SDSSJ2232-0744, with a color-based $T_{\rm eff}$ estimate near 6,500 K (i.e. not far from the hypothesized boundary for peculiar-DQ formation) fits nicely into this picture. However, the existence of three stars in Fig. 8 (as well as the GSC2 star mentioned above) that are redder, but have apparently normal C_2 bands, would require a significant range of H/He/C abundances in these stars.

The third star (SDSSJ1113+0146) and seventh star (SDSSJ1333+0016) both exhibit distorted spectra, both have counterparts in the literature with similar spectra, and both show significant circular polarization in data taken at the MMT. SDSSJ1113+0146 appears similar to LP 790-29, a star with a temperature 7,500 K exhibiting distorted and displaced carbon bands and strong polarization (Liebert et al. 1978; Wickramasinghe & Bessell 1979; Schmidt et al. 1999). Bues (1999) modeled that star with a field strength of 50 MG. SDSSJ1333+0016 has a spectrum with strong, scalloped carbon bands almost identical to the spectrum of LHS 2229 (Schmidt et al. 1999). These authors make the case that the displaced, rounded band features are more likely associated with those due to the hypothesized C₂H bands. Indeed, the energy distribution of LHS 2229 suggests that its T_{eff} is lower than 6300 K.

In summary, the new DQ stars found here show a transition from stars with atomic carbon to stars with molecular carbon that is correlated with color (and presumably temperature) as we would expect. However, the redder, cooler DQ stars have a wide range of C_2 band strength

at a given color, and the two reddest stars are probably as cool as any DQ stars, but appear to have "normal" C₂ bands. The interpretation is complicated by two good candidates for highly magnetic, polarized WDs showing distorted bands. No new detections of stars with CH features were made.

3.4. Metallic-lined DZ Stars

The occurrence of heavy elements — calcium, and sometimes also magnesium, iron, and other species — in cool helium WD atmospheres can result in quite strong spectral blanketing at primarily ultraviolet wavelengths. The origin of this additional opacity in a small fraction of cool non-DA WDs is believed to be interstellar or circumstellar accretion. When the absorption is sufficiently strong, the reddening of the u-r color can pull these stars out of the normal helium WD locus. For this class of WD, some of the stars found so far by SDSS substantially enrich the variety of spectra that are known.

Most DZ stars found in SDSS spectra exhibit only the Ca II H&K resonance doublet. There are five found in the 41-plate sample and listed in Table 2, although one (SDSSJ0944-0039) is hot enough to have He lines too and is classified as DBZ. Their spectra are shown in Figure 9, together with the brightest of the DC stars (with no detected features) from the 41-plate sample. That they are degenerate dwarfs and not subdwarfs is virtually guaranteed by the nondetections of such features as the Ca I 4227Å line, the 4300Å CH band, H β , the Mg I 5175Å triplet, and the Na I 5892Å resonance doublet. The energy distributions (flat g-i colors) suggest that these objects are warm; a Bergeron pure-He model of 9500 K has zero color. However, the pure-He models may overestimate the temperatures of DZ stars (Wolff et al. 2002). The wide range of Ca line strengths among these stars with similar colors is obvious. Although SDSSJ1610+0046 has weak Ca lines, it is classified DC: as the reddening is relatively high and the lines may be interstellar.

In Figure 10, ten spectra of DZ stars are shown that feature a detection of metallic lines other than calcium. Most of them show lines of Mg I at 3829, 3832, 3838, 5167, 5173, and 5184 Å, and several show the NaD lines at 5890 and 5896 Å. The Ca II lines at 3933 and 3968 Å are generally strong, and the CaI lines at 4226, 4335, and 4455 Å are often present. The CaII infrared triplet at 8498, 8542, and 8662 Å is clearly present in most of the warmer stars, although the noise in the spectra left after sky subtraction prevents seeing the lines in the fainter stars. The spectra are plotted in order of r-z color that is probably close to their order of temperature. The first three stars are the warmest, with temperatures 10000–12000 K, as indicated by their colors compared to the Bergeron models with pure He atmospheres. The next four spectra are redder, show generally stronger Mg lines (including lines of MgI at 4352, 4703, and 5528 Å, and perhaps of MgII at 4481 Å), and all show numerous lines of FeI — we return to them below. The third and fifth spectra (SDSSJ0939+5550 and SDSSJ0956+5912) also show Balmer lines and are DZA, an unusual type examplified by Ross 640 (Liebert 1977).

The last three spectra in Fig. 10 have unusual (and uncertain) classifications. The eighth (SDSSJ0157+0033) is noisy, but has a strong turnover of the blue spectrum, suggesting strong Ca (and perhaps Fe) absorption, as well as apparent complex structure of the probable Mg I detection. This structure is reminiscent of the spectrum of the only previously known magnetic DZ star, LHS 2534 (Reid et al. 2001). The spectrum of that star was most noteworthy for its strong, Zeeman-split Na I absorption, but the weaker Mg I lines were also split into several components. While the S/N ratio of the spectrum of SDSSJ0157+0033 is too modest for a detailed comparison, the most likely interpretation is that this star is also magnetic. The lack of distinct features at bluer wavelengths might also be explained by the magnetic hypothesis. Probable Ca I 4227Å appears unshifted in the spectrum, as it does in LHS 2534. A more distinct Ca II absorption appears in the LHS object, but both spectra turn over sharply below 4500Å.

The ninth spectrum in Fig. 10 (SDSSJ0135+1302) probably has very strong Ca absorption and weak, barely detected Mg absorption. It may have broad H α absorption, although that apparent feature may be an artifact of incorrect flux calibration. The tenth spectrum (SDSSJ1330+6435) appears to have extreme absorption by NaI (and possibly by Ca, but there is insufficient flux to tell). It appears to be very similar to that of the star 2356-2054 found in the proper-motion survey of Oppenheimer et al. (2001). We find SDSSJ1330+6435 also to have a non-zero proper motion, ruling out its interpretation as a broad absorption line QSO.

Returning now to the fourth to seventh spectra from Fig. 10, an expanded plot of the blue end of the spectra is shown in Figure 11, showing details not previously seen in DZ WDs. Detected lines of Ca, Mg, and Na are marked by open circles at the top of Fig. 11 (and their wavelengths are listed in the text above), and some detected lines of FeI are marked by small filled circles. These FeI lines come from multiplet numbers 4, 15, 41, 42, 43, 45, but more lines from other multiplets are probably present as well. It is useful to compare these four spectra to lend confidence that many weak features are real. Many are also present in the strongly blanketed DZ star G 165-7. The FeI lines are barely resolved (FWHM ~4Å in unsmoothed spectra), and Ca I 4227Å is also prominent and only slightly broader (FWHM \sim 7Å). MgI presents itself in a variety of strengths, indicating for SDSSJ0956+5912 and SDSSJ0937+5228 a remarkably strong MgI strength relative to the apparent Ca II strength. The asymmetry in the strong Mg I lines due to the extended blue wings has been seen before in G 165-7 (Hintzen & Strittmatter 1974). Wehrse & Liebert (1980) argued that the asymmetry is explained by fitting a model profile assuming a static theory, rather than the usual impact approximation, for the van der Waals broadening in a neutral helium-dominated atmosphere. Traving (1968) has demonstrated such an asymmetry in laboratory measurements.

In contrast to the fairly sharp lines of FeI and CaI in Fig. 11, the Fe I features in previous spectra of WDs are broader, and often hopelessly blended. They contribute to the reddening of the spectrum below 4500Å in the strong-DZ stars vMa 2 (Greenstein 1960) and G 165-7. To what can we attribute the contrast between the sharp metallic lines in Fig. 11 and the previous objects? A temperature difference is one possibility. G 165-7 has an inferred $T_{\rm eff}$ of 7,500 K

(Wehrse & Liebert 1980), while several crude estimates suggest a temperature for vMa 2 near 6,000 K. Cool WDs have higher-pressure atmospheres and greater line broadening, and the SDSS objects could be somewhat warmer. It has previously been suggested that cool WDs with hydrogen-dominated atmospheres could indeed show narrow metallic lines (Hintzen & Strittmatter 1975). SDSSJ0956+5912 does show up to three Balmer lines. The presence of hydrogen in the atmosphere may greatly increase the opacity while decreasing the pressures where lines are formed in the atmosphere. Only a detailed analysis of these spectra can show what the temperatures and abundances are. The breadth of the Ca II lines and the asymmetric Mg I profiles leave little doubt that they are degenerate dwarfs, rather than some kind of peculiar subdwarfs.

3.5. Hot subdwarfs

There are at least two spectral classes of these stars with lower gravity than WDs (but not as low as horizontal branch stars or main-sequence F stars), called subdwarf B (sdB) and subdwarf O (sdO). The former show primarily hydrogen lines, generally with helium weak or absent (and sub-solar in abundance due to diffusion). The generally accepted interpretation of these stars is that they are core helium-burning stars which have somehow been stripped of virtually all of the overlying hydrogen-rich envelope. They are field analogs to extreme horizontal branch (EHB) stars found in old, especially metal-poor globular clusters. One might therefore expect a temperature sequence of sdB/EHB stars to link to the blue horizontal branch (BHB) stars which occupy a well-defined, unique position in Sloan color-color diagrams (Yanny et al. 2000). However, there is a known class of helium-rich stars similar in temperature to the sdB stars called He-sdB stars.

The 38 sdB and 18 sdO stars found in the 41-plate sample are listed in Table 3. They do not lie on a well-defined sequence of colors (Fig. 1), but scatter throughout and around the colors of the hot WDs. The spectra of the brightest eleven stars are shown in Figure 12. Some exhibit strong helium lines in the spectra, and are likely related to the hotter sdO or helium-rich He-sdB stars. For a few stars here, the quality of the spectrum is too poor to classify the object at all. This heterogeneous group includes objects evolved beyond the core helium-burning phase. It is too early for a systematic assessment of sdB, sdO, and other hot, lower gravity stars in SDSS. However, the substantial number listed in Table 3 shows that the survey will ultimately allow an extensive classification and discussion of these stars.

4. Discussion

Some comparison can be made between this paper and WDs discovered previously. A cross-check with the NLTT Catalogue (Luyten 1979) shows reasonable consistency. There are eight stars in Tables 1–3 that have a proper motion >180 mas yr⁻¹ and are bright enough (g < 19) that they are likely to be included in the NLTT. All but one (the DA4 star SDSSJ1258+0007) are

in the NLTT with a proper motion close to the motion found here.

The McCook & Sion (1999) catalog lists 38 WDs in the region of the 41-plate sample. Six additional WDs in our 41-plate sample in Tables 1 and 2 have been identified in the Hamburg/ESO Survey (Koester et al. 2001; Christlieb et al. 2001) or in the Hamburg Quasar Survey (Homeier et al. 1998; Homeier 2002, private communication) and are noted in the tables. Of these 44 WDs, 14 have spectra taken here, and the spectral types agree very well. (The star WD1352+004 was classified DB4, but here is found to have Balmer absorption and is called DBA4.) Most of the remaining stars can be identified in the imaging data, but did not get spectroscopic fibers assigned. Our spectroscopic identification of 269 WDs in this region is an increase by a factor of more than six over the WDs known previously, and gives some indication of the returns that can be expected from the complete survey. Our "complete" region has 10 square degrees of overlap with the 15-hour field of Evans (1992). Evans finds 12 WDs in this overlap region from his reduced proper motions. We have spectra taken of five (3 DB, 1 DA, 1 DA+M), and we have spectra of an additional 12 WDs that Evans did not find — 10 with their proper motions below his lower limit and 2 apparently too faint. Again, SDSS is yielding greater returns in the WDs identified.

With the WDs and hot subdwarfs in Tables 1–3 inside the 41-plate area (omitting the stars in Table 2 outside this area), we can look at the density on the sky of these hot stars. Let us consider two subsamples: hot stars with $(u-g)_0 < 0.0$ and $(g-r)_0 < -0.2$, and medium-hot stars with $0.0 < (u - g)_0 < 0.6$ and $(g - r)_0 < -0.2$. These subsamples need to be considered separately because a higher priority is given for fiber assignment to the "HOT_STANDARD" stars with the bluer colors. These two groups contain DA WDs with roughly T > 22000 and 12000 < T < 22000 K, respectively. Taking stars with 15 < g < 20, and applying the full reddening corrections (which is not correct for some of the brightest and reddest nearby WDs, but which will not affect the conclusions), a summary is given in Tables 4 and 5. In these tables, columns 2 and 3 give the number of stars with observed spectra, and columns 4 and 5 give the corresponding density on the sky. However, SDSS only targets some fraction of all hot stars for spectroscopic observations; the fraction can be estimated by counting objects in the SDSS imaging catalogs with stellar image profiles and with the same magnitude and color limits as above. The blue stars without spectra are assumed to have the same DA/DB/sdB distributions found from the stars with spectra in each color subsample at each magnitude. Then the densities in columns 4 and 5 can be adjusted to give the total sky densities. The last columns in Tables 4 and 5 give these results for the total density on the sky of blue stars with 15 < g < 20 adjusted for incomplete selection for obtaining spectra. The tables show that for brighter, hot stars (g < 19and $(u-g)_0 < 0.0$), most stars have SDSS spectra. For fainter stars and for the medium-hot subsample, the fraction with spectra is roughly one-third.

The density of WDs found here is consistent with simulations (Fan 1999) of 5 deg⁻¹ for WDs of all temperatures with 15 < g < 20 at b=60°. The hot sdB/sdO stars outnumber hot WDs at bright magnitudes, as was also found in the PG Survey Green et al. (1986). The numbers reverse at fainter magnitudes, however, as the space density of sdB stars drops at large distances from

the Galactic plane. The reversal can be seen in Table 5, where the numbers of WDs and hot subdwarfs are shown from the hot-star subsample with $(u-g)_0 < 0.0$ and $(g-r)_0 < -0.2$. The star densities in Tables 4 and 5 will vary with Galactic latitude — the latitude dependence will be explored when larger SDSS samples are available.

At cooler temperatures (6000–10000 K), WDs are still separated in color from main-sequence stars, and many can be identified using a combination of color and proper-motion selection. For yet-cooler temperatures (4000–6000 K), proper motion will be essential to isolate WDs, and even then contamination from metal-poor halo subdwarf stars will be a severe difficulty. Finally, WDs at temperatures below 4000 K have their red-IR flux depressed by molecular hydrogen absorption (collision induced absorption). Their SDSS colors then become so distorted that they are easily identified. Stars SDSSJ1337+0001 and LHS3250 (Harris et al. 2001) are seen to be prominant outliers in Fig. 1b and Table 2 — they are still the only stars of this type discovered or recovered in the SDSS. Future papers will discuss these rare stars further as more are found.

Funding for the Sloan Digital Sky Survey (SDSS) has been provided by the Alfred P. Sloan Foundation, the Participating Institutions, the National Aeronautics and Space Administration, the National Science Foundation, the U.S. Department of Energy, the Japanese Monbukagakusho, and the Max Planck Society. The SDSS is a joint project of The University of Chicago, Fermilab, the Institute for Advanced Study, the Japan Participation Group, The Johns Hopkins University, Los Alamos National Laboratory, the Max-Planck-Institute for Astronomy (MPIA), the Max-Planck-Institute for Astrophysics (MPA), New Mexico State University, University of Pittsburgh, Princeton University, the United States Naval Observatory, and the University of Washington. We are grateful to P. Bergeron for calculating SDSS colors of WD models, and D. Homeier for providing lists of WDs from the Hamburg Survey in advance of publication. SLH, NMS, and PS acknowledge support from NSF grant AST 0205875. Studies of strongly magnetic stars and stellar systems at Steward Observatory are supported by NSF grant AST 97-30792 to GS.

REFERENCES

Bergeron, P., Leggett, S.K., & Ruiz, M.T. 2001, ApJS, 133, 413

Bergeron, P., Saffer, R.A., & Liebert, J. 1992, ApJ, 394, 228

Bergeron, P., Wesemael, F., & Beauchamp, A. 1995, PASP, 107, 1047

Boyle, B.J. 1989 MNRAS, 240, 533

Bues, I. 1999, in Eleventh European Workshop on White Dwarfs, ed. J.E. Solheim & E.G. Meistas (San Francisco: ASP), 240

Carollo, D., Hodgkin, S.T., Spagna, A., Smart, R.L., Lattanzi, M.G., McLean, B.J., & Pinfield, D.J. 2002, A&A, 393, 45

Carollo, D., Koester, D., Spagna, A., Lattanzi, M.G., & Hodgkin, S.T. 2003, A&A, in press, astro-ph/0301648

Christlieb, N., Wisotzki, L., Reimers, D., Homeier, D., Koester, D., & Heber, U. 2001, A&A, 366, 898

Darling G.W., & Wegner, G. 1996, AJ, 111, 865

Dreizler, S., & Werner, K. 1996, A&A, 314, 217

Eggen, O.J., & Greenstein, J.L. 1965, ApJ, 141, 83

Evans, D.W. 1992, MNRAS, 255, 521

Fan, X. 1999, AJ, 117, 2528

Finlator, K., et al. 2000, AJ, 120, 2615

Fleming, T.A., Liebert, J., & Green, R.F. 1986, ApJ, 308, 176

Fukugita, M., Ichikawa, T., Gunn, J.E., Doi, M., Shimasaku, K., & Schneider, D.P. 1996, AJ, 111, 1748

Gänsicke, B.T., Euchner, F., & Jordan, S. 2002, A&A, in press, astro-ph/0208454

Graham, J.A. 1972, AJ, 77, 144

Green, R.F., Schmidt, M., & Liebert, J. 1986, ApJS, 304, 867 (PG)

Greenstein, J.L. 1960, in Stellar Atmospheres, ed. J.L. Greenstein, (Chicago, Univ. of Chicago), 161

Gunn, J.E., et al. 1998, AJ, 116, 3040

Harris, H.C., et al. 2001, ApJ, 549, L109

Hintzen, P., & Strittmatter, P.A. 1974, ApJ, 193, L111

Hintzen, P., & Strittmatter, P.A. 1975, ApJ, 201, L37

Hogg, D.W., Finkbeiner, D.P., Schlegel, D.J., & Gunn, J.E. 2001, AJ, 122, 2129

Homeier, D., Koester, D., Hagen, H.-J., Jordan, S., Heber, U., Engels, D., Reimers, D., & Dreizler, S. 1998, A&A, 338, 563

Kemic, S.B. 1974, JILA Report 113

Koester, D., et al. 2001, A&A, 378, 556

Krisciunas, K., Margon, B., & Szkody, P. 1998, PASP, 110, 1342

Lenz, D.D., Newberg, H.J., Rosner, R., Richards, G.T., & Stoughton, C. 1998, ApJS, 119, 121

Liebert, J. 1977, A&A, 60, 101

Liebert, J., Angel, J.R., Stockman, H.S., & Beaver, E.A. 1978, ApJ, 225, 181

Luyten, W.J. 1976, A Catalogue of Stars with Proper Motions Exceeding 0.5" Annually (Minneapolis: Univ. Minnesota Press) (LHS)

Luyten, W.J. 1979, NLTT Catalogue (Minneapolis: Univ. Minnesota Press) (NLTT)

McCook, G.P. & Sion, E.M. 1999 ApJS, 121, 1

Monet, D.G., et al. 1999, The USNO-A2.0 Catalog, http://www.nofs.navy.mil/projects/pmm/a2.html

Monet, D.G., et al. 2003, AJ, 125, 984

Nitta, A., Kleinman, S.J., Krzesinski, J., Harris, H.C., Liebert, J., & Eisenstein D. 2003, in White Dwarfs, ed. D. deMartino & R. Silvotti (London: NATO), in press

Oppenheimer, B.R., Hambly, N.C., Digby, A.P., Hodgkin, S.T., & Saumon, D. 2001, Science, 292, 698

Pelletier, C., Fontaine, G., Wesemael, F., Michaud, G., & Wegner, G. 1986, ApJ, 307 242

Pier, J.R., Munn, J.A., Hindsley, R.B., Hennessy, G.S., Kent, S.M., Lupton, R.H., & Ivezić, Z. 2003, AJ, 125, 1559

Pottasch, S.R. 1996, A&A, 307, 561

Raymond, S.N., et al. 2003, AJ, in press, astro-ph/0302405

Reid, I.N., Liebert, J., & Schmidt, G.D. 2001, ApJ, 550, L61

Reimers, D., Jordan, S., Beckmann, V., Christlieb, N., & Wisotzki, L. 1998, A&A, 337, L13

Richards, G.T., et al. 2002, AJ, 123, 2945

Salaris, M., Domínguez, I., García-Berro, E., Hernanz, M., Isern, J., & Mochkovitch, R. 1997, ApJ, 486, 413

Schlegel, D.J., Finkbeiner, D.P., & Davis, M. 1998, ApJ, 500, 525

Schmidt, G.D., Bergeron, P., & Fegley, Jr., B. 1995, ApJ, 443, 274

Schmidt, G.D., Liebert, J., Harris, H.C., Dahn, C.C., & Leggett, S.K. 1999, ApJ, 512, 916

Schmidt, G.D., Vennes, S., Wickramasinghe, D.T., & Ferrario, L. 2001, MNRAS, 328, 203

Schmidt, G.D., et al. 2003, ApJ, submitted

Sion, E.M., Greenstein, J.L., Landstreet, J.D., Liebert, J., Shipman, H.L., & Wegner, G. 1983, ApJ, 269, 253

Smith, J.A., et al. 2002, AJ, 123, 2121

Stoughton, C., et al. 2002, AJ, 123, 485

Szkody, P., et al. 2002, AJ, 123, 430

Traving, G. 1968, in Plasma Diagnostics, ed. W. Lochte-Holtgreven (Amsterdam: North Holland Publishing Company)

Wegner, G. 1979, AJ, 84, 1384

Wegner, G., & Yackovich, F.H. 1984, ApJ, 284, 257

Wehrse, R., & Liebert, J. 1980, A&A, 86, 139

Wesemael, F., Greenstein, J.L., Liebert, J., Lamontagne, R., Fontaine, G., Bergeron, P., & Glaspey, J.W. 1993, PASP, 105, 761

Wickramasinghe, D.T., & Bessell, M.S. 1979, MNRAS, 188, 841

Wickramasinghe, D.T., & Ferrario, L. 1988, ApJ, 327, 222

Wolff, B., Koester, D., & Liebert, J. 2002, A&A, 385, 995

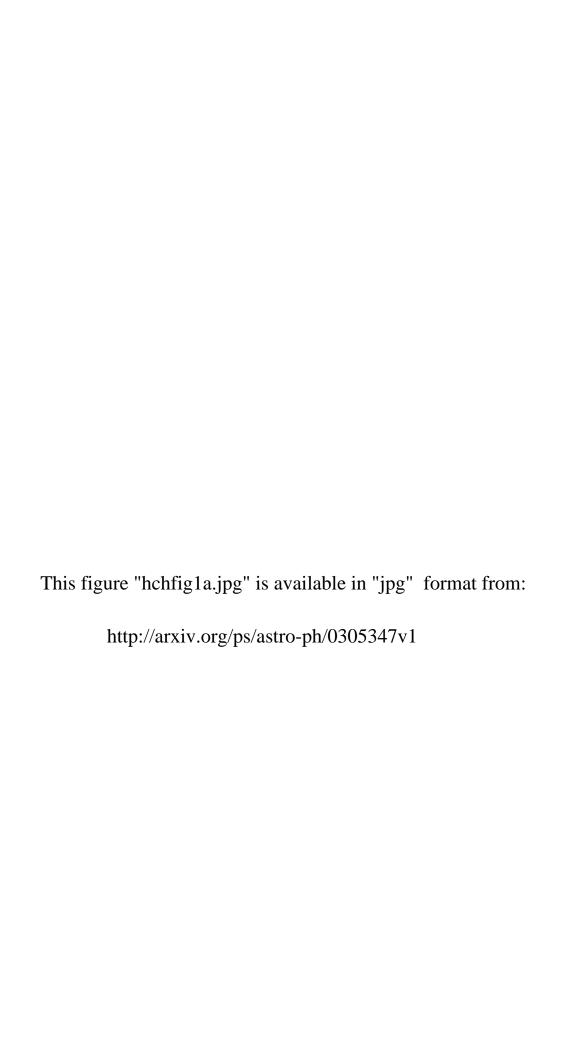
Yanny, B., et al. 2000, ApJ, 540, 825

York, D.G., et al. 2000, AJ, 120, 1579

This preprint was prepared with the AAS LATEX macros v4.0.

- Fig. 1.— Color-color diagrams (u-g/g-r) in panel (a), g-r/r-i in panel (b)) showing the WDs and hot subdwarfs in Tables 1–3. Different types are shown with different symbols. Small dots show all objects with stellar image profiles with 15 < g < 20 in a region of 25 deg². The curves show the colors of WD model atmospheres (Bergeron et al. (1995)) of pure H (solid curves) and pure He (dashed curves) with $\log g = 7$, 8, and 9, where the $\log g = 7$ curve is toward the lower right and the $\log g = 9$ curve is toward the upper left in panel (a). The dotted lines with labels connect models with the same effective temperature.
- Fig. 2.— Sequence of DA4 stars covering a range of magnitudes. The g magnitude is given at the left below each spectrum. The coordinates (and in parentheses, the plate–fiber number of the spectrum) are given at the right below each spectrum. The spectra in this and following figures have been smoothed by 5 pixels to a resolution of about 1200.
- Fig. 3.— A sample of DA WDs with hydrogen atmospheres, arranged in order of u i color and spectral type. DA stars cooler than DA7 (7000 K) exist, but are not targeted for SDSS spectra because their colors overlap with the stellar locus.
- Fig. 4.— A sample of hot WDs with helium atmospheres, arranged in order of u i color. The first two are DO and the last five are DB, except the sixth has hydrogen (weak H β , stronger H α) and is DBA.
- Fig. 5.— Twelve magnetic DAH stars, arranged in order of increasing field strength.
- Fig. 6.— Three magnetic DBH stars.
- Fig. 7.— Ten DQ stars with weak carbon features, plotted in order of u i color. The first four stars show the atomic lines of CI marked by dots at the top of the plot. The fourth and following stars show the Swan bands of molecular carbon. The heads of the three strongest (1,0), (0,0), and (0,1) bands are marked by dashed lines.
- Fig. 8.— Nine DQ stars with strong Swan bands of molecular carbon, plotted in order of u i color. The heads of the three strongest bands are marked by dashed lines.
- Fig. 9.— Sequence of all DZ stars and the brighter DC stars in the 41-plate sample, plotted in order of g i color. The top spectrum shows a DBZ star with He and Ca. The remaining eight spectra show four typical DZ stars, with Ca but no other elements detected, and four DC stars with no definite features.
- Fig. 10.— Sequence of ten DZ stars with Mg and/or Na lines present, in addition to Ca. They are plotted in order of r-z color.
- Fig. 11.— Blowup of four DZ spectra from Fig. 10 showing a rich set of metallic lines. The wavelengths of some of the detected lines are marked at the top by open circles (Ca and Mg lines) and small filled circles (Fe lines).

Fig. 12.— The brightest of the hot subdwarfs with g < 16.7, arranged by u - i color with bluer stars at the top.



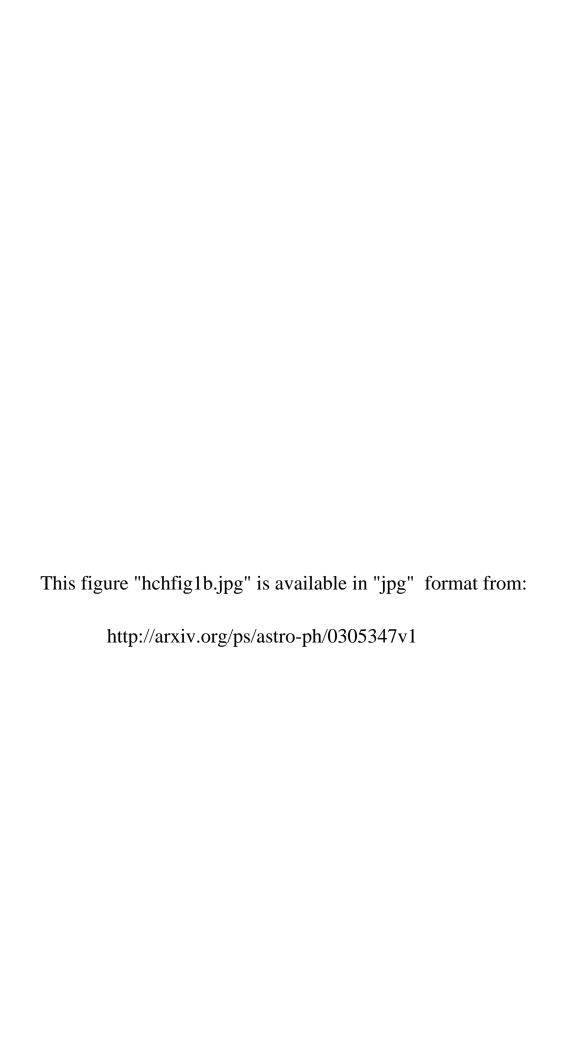


Table 1. DA and DB White Dwarfs $\,$

=	Name SDSS J+	g	u-g	g-r	r-i	i-z	A_u	$\mu \pmod{\operatorname{yr}}$	PA (deg)	Spec. Type	Note
	09 41 07.47-00 19 49.8	18.96	0.43	-0.15	-0.16	-0.21	0.31	18		DA:	_
	$09\ 41\ 35.45{-}00\ 09\ 17.1$	19.35	-0.41	-0.44	-0.36	-0.11	0.34	11		DA1:	
	$09\ 41\ 52.14{+}00\ 16\ 39.8$	18.47	0.01	-0.39	-0.28	-0.31	0.48	28	177	DA3	
	$09\ 43\ 23.70{+}00\ 55\ 34.0$	19.30	0.23	-0.28	-0.40	0.24	0.70	25	248	DA3.5	
	09 45 53.60-00 35 04.2	19.35	0.48	0.15	0.03	-0.11	0.46	57	234	DA6:	
	09 46 40.35+01 13 19.9	17.18	0.11	-0.37	-0.24	-0.25	0.75	33	261	DA3.5	1
	09 48 04.31-00 07 38.3	18.28	0.42	-0.06	-0.13	-0.14	0.52	49	270	DA6	
	$09\ 48\ 22.02{-}00\ 04\ 38.5$	20.06	0.42	-0.27	-0.22	-0.54	0.48	20	243	DA4	
	09 48 44.84+00 35 16.7	17.73	0.27	-0.15	-0.18	-0.30	0.40	89	243	DA4	
	09 49 01.28-00 19 09.5	16.51	0.46	-0.16	-0.18	-0.13	0.39	112	141	DA4	
	09 49 17.05-00 00 23.7	18.80	0.45	-0.13	-0.17	-0.19	0.40	50	192	DA5	
	09 50 27.87+00 05 35.7	18.49	-0.07	-0.35	-0.28	-0.24	0.30	12		DB2	
	$09\ 50\ 42.11 + 01\ 15\ 26.5$	17.87	0.00	-0.39	-0.26	-0.23	0.25	47	251	DA3	
	09 51 02.23+01 04 32.6	15.59	-0.12	-0.36	-0.20	-0.29	0.31	79	244	DB3	2
	$09\ 53\ 29.20{-}00\ 51\ 00.6$	18.85	0.40	-0.06	-0.11	-0.10	0.17	36	290	DA5	
	09 58 10.68-01 04 17.8	16.51	-0.11	-0.33	-0.33	-0.23	0.21	21	248	DA2.5	3
	09 59 40.23+00 36 34.0	18.50	0.41	-0.31	-0.14	-0.15	0.13	38	149	DA4	
	$10\ 03\ 16.36{-00}\ 23\ 37.0$	15.96	0.01	-0.35	-0.26	-0.28	0.24	55	249	DA2.5	4
	10 06 09.18+00 44 17.1	17.86	0.46	0.16	0.34	0.67	0.19	51	285	DA7+M	
	$11\ 10\ 28.71{-}00\ 33\ 43.5$	18.61	0.42	-0.05	-0.07	-0.15	0.20	83	271	DA5	
	11 13 22.91+00 05 31.0	19.66	-0.29	-0.60	-0.28	-0.05	0.24	< 20		DA:	
	11 17 01.97+00 03 23.0	18.81	0.06	-0.37	-0.26	-0.22	0.22	6		DA4:	
	11 20 04.00-00 23 23.1	20.26	0.36	-0.12	-0.26	-0.66	0.18	9		DA5:	
	$11\ 23\ 07.37 + 00\ 32\ 16.2$	19.43	0.24	-0.05	0.65	0.58	0.17	18		DA5:+M	5
	11 23 57.72-01 10 27.5	17.95	0.03	-0.29	0.22	0.45	0.31	22	167	DA3:+M	5
	$11\ 26\ 13.52{-00}\ 21\ 09.8$	17.99	0.14	-0.28	-0.26	-0.31	0.13	29	215	DA4:	
	11 26 23.86+01 08 57.0	18.74	0.45	0.53	0.83	0.50	0.17	20	242	DA4:+M	5
	$11\ 26\ 40.15{+}00\ 23\ 47.0$	18.85	-0.27	-0.44	-0.29	-0.11	0.17	16		DA2.5	
	11 27 12.17+00 16 44.3	19.73	0.38	-0.17	-0.20	-0.28	0.17	28	274	DA5	
	$11\ 27\ 48.26{-00}\ 28\ 59.9$	18.28	0.31	-0.21	0.22	0.74	0.16	36	254	DA4.5+M	5
	11 32 13.00-00 30 36.8	19.84	0.38	-0.22	-0.20	-0.29	0.12	21	319	DA5:	
	11 33 54.12+00 18 45.7	20.42	0.04	-0.32	-0.35	-0.61	0.11	20	104	DA4:	
	11 34 07.24-00 45 13.0	20.27	0.06	-0.39	-0.24	-0.38	0.11	16		DA3:	
	11 36 14.89+00 51 06.9	19.13	0.47	-0.06	-0.13	-0.06	0.12	31	269	DA6	
	11 36 56.33+00 58 35.5	18.85	-0.19	-0.44	-0.37	-0.17	0.12	17		DA2.5	
	$11\ 37\ 09.84 + 00\ 35\ 42.9$	18.51	0.25	-0.28	-0.19	-0.22	0.12	20	223	DA4	
	$11\ 37\ 25.16{-00}\ 22\ 59.2$	18.03	0.48	0.00	0.03	-0.11	0.10	29	177	DA6	
	$11\ 37\ 38.38{-00}\ 27\ 21.7$	17.96	0.36	0.07	-0.06	-0.08	0.10	106	301	DA4	
	$11\ 37\ 48.31{-}00\ 27\ 14.7$	19.35	0.25	-0.29	-0.29	-0.10	0.09	16		DA4	
	$11\ 38\ 00.35{-}00\ 11\ 44.5$	18.86	0.35	-0.01	0.71	0.62	0.10	18		DA5:+M	5
	11 39 01.22+00 03 21.8	18.87	0.28	-0.20	-0.16	-0.22	0.12	13		DA:	
	11 39 41.32-00 40 09.8	17.67	-0.04	-0.45	-0.27	-0.31	0.07	28	143	DA3	
	$11\ 40\ 10.54{-00}\ 29\ 35.5$	19.81	-0.01	-0.21	-0.26	-0.07	0.09	< 20		DB4	
	$11\ 40\ 26.12{+00}\ 12\ 18.6$	19.27	0.41	-0.22	-0.15	-0.30	0.14	28	210	DA:	
	$11\ 43\ 12.58{+00}\ 09\ 26.6$	18.15	0.27	-0.07	0.58	0.60	0.13	28	236	DA3:+M	5
	$11\ 44\ 43.93{-}01\ 01\ 44.6$	19.13	0.54	0.15	-0.02	0.05	0.10	59	244	DA7	
	$11\ 46\ 05.39{+}00\ 14\ 58.6$	19.68	-0.05	-0.22	-0.18	-1.06	0.15	21	106	DB4:	
	$11\ 46\ 08.73{-00}\ 24\ 39.2$	18.08	-0.31	-0.35	-0.36	-0.26	0.13	26	219	DA2.5	
	$11\ 46\ 24.47{-00}\ 28\ 22.8$	19.56	0.22	-0.34	-0.24	-0.24	0.14	29	309	DA4	
	$11\ 47\ 20.41{-00}\ 24\ 05.8$	18.42	0.14	-0.23	-0.25	-0.39	0.16	32	231	DA3.5	
	$11\ 47\ 51.73{+}00\ 17\ 01.3$	19.81	-0.11	-0.31	-0.20	-0.10	0.15	2		DB4	
	$11\ 47\ 56.01{+}00\ 43\ 40.8$	18.15	0.45	-0.06	-0.10	-0.16	0.15	18		DA5	

Table 1. (continued)

Name SDSS J+	g	u-g	g-r	r-i	i-z	A_u	μ (mas/yr)	PA (deg)	Spec. Type	Note
11 51 05.83-00 11 35.9	19.13	0.54	0.19	0.03	0.03	0.11	49	198	DA7	
$11\ 51\ 56.95{-00}\ 07\ 25.5$	18.14	0.50	-0.02	0.33	0.51	0.13	64	116	DA5+M	5
11 52 36.99+00 21 41.8	17.30	0.51	-0.06	0.04	0.16	0.12	20	307	DA5+M	
$12\ 38\ 36.35{-00}\ 40\ 42.3$	17.40	-0.36	-0.35	0.02	0.23	0.11	21	166	DA1+M	6
12 39 22.33+00 55 48.8	19.27	0.32	0.06	0.81	0.62	0.09	21	165	DA4:+M	5
$12\ 44\ 51.38{-00}\ 10\ 45.7$	19.84	0.03	-0.28	-0.20	-0.32	0.10	10		DB4.5	
12 47 09.83+00 55 33.0	19.37	0.13	-0.33	-0.27	-0.25	0.10	2		DA4	
12 47 48.90-01 11 09.9	16.97	0.51	0.18	0.00	-0.02	0.12	~ 300	150	DA7	7
12 49 20.09+00 19 11.6	19.72	-0.02	-0.44	-0.31	-0.22	0.12	18		DA3	
$12\ 49\ 59.11{-}00\ 51\ 02.0$	19.01	0.45	0.08	-0.02	-0.10	0.13	81	208	DA7:	
12 51 09.24+00 43 21.0	20.24	0.39	-0.21	0.57	0.62	0.10	15		DA4+M	8
12 51 25.95+00 26 40.1	20.07	0.23	-0.31	-0.26	-0.30	0.09	17		DA4	
12 51 39.79-01 02 54.1	18.38	0.46	-0.13	-0.09	-0.17	0.16	52	271	DA5	
12 52 14.27-00 50 57.6	17.25	0.41	-0.25	-0.22	-0.25	0.14	106	282	DA4	
12 53 12.11+00 55 42.7	20.36	0.07	-0.34	-0.41	-0.08	0.11	< 20		DA:	
12 53 18.91+00 04 23.5	19.75	0.50	-0.20	-0.11	-0.28	0.12	35	239	DA4.5	
12 53 55.28+00 14 29.4	18.96	0.45	-0.22	-0.18	-0.16	0.12	24	206	DA4.5	
12 53 57.87-00 54 43.0	19.39	0.42	0.03	0.03	-0.19	0.11	65	282	DA7	
12 54 24.67+00 28 18.9	19.84	0.44	-0.05	-0.17	-0.16	0.11	30	115	DA6	
12 54 27.48+01 01 51.9	19.33	0.41	-0.30	-0.21	-0.34	0.10	14		DA4	
12 56 52.84-00 01 10.7	19.24	0.42	-0.19	-0.24	-0.23	0.10	14		DA4.5	
12 57 20.78-01 03 09.1	18.07	0.44	-0.11	-0.16	-0.19	0.11	23	223	DA5	
12 57 30.32-00 11 51.0	18.79	-0.18	-0.50	-0.24	-0.25	0.12	15		DA3	
12 58 16.99+00 07 10.2	18.15	0.30	-0.29	-0.21	-0.39	0.11	287	243	DA4	
13 01 10.51+01 07 39.7	16.30	0.40	-0.14	-0.17	-0.18	0.12	24	83	DA4.5	9
13 02 11.77+00 47 26.7	19.09	0.45	-0.26	-0.19	-0.13	0.12	83	276	DA4	-
13 17 24.75+00 02 37.3	15.77	-0.48	-0.55	-0.38	-0.37	0.14	22	297	DO	10
13 20 44.69+00 18 55.0	17.14	-0.01	-0.34	-0.22	-0.32	0.12	44	254	DA2.5	-
13 23 40.35+00 33 38.8	18.51	0.42	0.08	0.00	-0.10	0.12	32	224	DA6.5	
13 23 50.27+01 03 04.2	18.50	0.30	-0.17	-0.17	-0.18	0.12	44	270	DA3	
13 24 01.80+00 47 44.3	18.09	-0.15	-0.41	-0.31	-0.33	0.12	34	177	DA2	
13 29 28.22-00 55 00.6	18.62	0.37	0.00	-0.08	-0.23	0.16	75	264	DA5	
13 29 44.38+00 28 36.3	19.80	-0.12	-0.34	-0.26	-0.47	0.14	21	272	DB:	
13 29 46.54+00 42 29.8	19.22	0.34	-0.06	-0.14	-0.32	0.14	20	252	DA4	
13 30 06.88+00 58 45.3	20.30	0.12	-0.21	-0.30	-0.18	0.14	12		DA:	
13 30 15.15+00 03 29.8	18.04	0.29	-0.29	-0.23	-0.28	0.13	55	253	DA3	
13 31 00.61+00 40 33.5	18.98	0.28	-0.30	-0.24	-0.34	0.14	45	233	DA3-4	
13 31 37.05+01 06 32.2	17.43	-0.32	-0.49	-0.33	-0.28	0.14	37	204	DA1.5	11
13 37 14.44+01 04 43.8	18.57	0.32	-0.11	-0.17	-0.11	0.11	19	201	DA4	11
13 38 31.75-00 23 28.0	17.09	0.45	-0.18	-0.18	-0.24	0.16	69	117	DA4	
13 38 38.49-00 07 12.6	18.70	0.35	-0.11	-0.11	-0.18	0.13	58	283	DA4	12
13 39 26.10+00 26 41.5	19.23	0.46	-0.14	-0.25	-0.23	0.16	16	200	DA4	12
13 39 47.74-00 20 03.6	18.12	0.46	0.14	0.23	-0.12	0.18	30	102	DA6.5	
13 41 20.87+00 42 04.7	19.74	-0.06	-0.22	-0.26	-0.08	0.15	29	134	DB4	
13 41 54.39+00 56 00.9	18.62	0.16	-0.33	-0.20	0.09	0.16	$\frac{25}{25}$	263	DA2	
13 42 36.48+00 47 43.1	18.89	0.10	-0.30	-0.20 -0.21	-0.40	0.15	37	287	DA2 DA3	
13 45 50.93-00 55 36.5	16.70	0.39 0.38	-0.30 -0.17	-0.21 -0.18	-0.40 -0.26	0.13 0.14	90	268	DA3 DA4	
13 46 05.90-00 41 56.1	18.77	0.38 0.42	-0.17 -0.10	-0.18 -0.14	-0.20 -0.22	0.14 0.14	$\frac{90}{24}$	337	DA4 DA5	
13 47 34.83-00 52 26.6	17.38	$0.42 \\ 0.04$	-0.10 -0.34	-0.14 -0.28	-0.22 -0.25	0.14 0.14	38	337 290	DA3 DA2-3	
								290		
13 48 20.41-01 12 24.8	18.42	-0.26	-0.43	-0.30	-0.26	0.20	8 7		DA1-2 DA3	
13 51 38.10-00 26 48.8	19.50	0.27	-0.29	-0.18	-0.15	0.18	7	116		
13 53 08.21+00 36 10.3	19.02	0.32	-0.26	-0.27	-0.26	0.20	34	116	DA3	

Table 1. (continued)

Name SDSS J+	g	u-g	g-r	r-i	i-z	A_u	$\mu \pmod{\operatorname{yr}}$	PA (deg)	Spec. Type	Note
13 54 59.88+01 08 19.2	16.36	0.42	-0.17	-0.17	-0.23	0.16	134	258	DA4	13
$13\ 55\ 32.41{+}00\ 11\ 24.0$	15.70	0.02	-0.28	-0.19	-0.23	0.21	62	225	DBA4	14
13 55 39.90-01 14 06.7	18.55	0.36	-0.25	-0.25	-0.21	0.23	27	159	DA3	
$13\ 56\ 10.32{-}00\ 22\ 30.7$	19.38	-0.17	-0.28	-0.30	-0.17	0.22	15		DB3	
$13\ 56\ 42.32{-00}\ 35\ 49.9$	20.44	0.35	-0.26	-0.35	-0.24	0.22	< 20		DA3:	
$13\ 57\ 00.58{+}01\ 12\ 20.8$	19.17	0.30	-0.23	-0.24	-0.22	0.18	39	257	DA3	
$13\ 58\ 48.22{+}01\ 01\ 00.3$	19.47	0.21	-0.25	-0.24	-0.21	0.18	9		DA2-3	
$13\ 59\ 25.32{-}00\ 34\ 26.6$	16.80	0.39	-0.12	-0.13	-0.20	0.20	103	311	DA4	
$14\ 03\ 27.76+00\ 21\ 19.5$	16.86	-0.45	-0.52	-0.36	-0.31	0.20	16		DA1	
$14\ 03\ 41.35 + 00\ 35\ 41.0$	20.03	0.26	-0.21	-0.21	-0.25	0.18	21	236	DA3	
$14\ 07\ 01.61{+}00\ 30\ 08.6$	17.59	0.40	-0.08	-0.13	-0.18	0.23	82	288	DA5	
14 07 23.03+00 38 41.9	17.68	0.02	-0.07	0.73	0.60	0.20	22	270	DA3+M	5
14 08 14.64+00 38 39.0	19.20	-0.19	-0.40	-0.25	-0.12	0.18	41	270	DB2	
14 13 22.39-00 14 51.6	18.00	0.30	-0.07	-0.15	-0.16	0.23	72	193	DA3	
14 13 56.52-00 26 43.2	17.44	0.38	-0.05	-0.10	-0.11	0.22	94	275	DA4	
14 15 16.11-01 09 12.1	18.27	0.22	-0.02	-0.09	-0.18	0.21	40	268	DA7:	
14 17 08.81+00 58 27.2	18.03	0.46	-0.21	-0.13	-0.13	0.19	33	267	DA3	
$14\ 17\ 47.96{-00}\ 05\ 49.6$	18.41	0.26	-0.26	-0.26	-0.32	0.20	18		DA3.5	
14 18 40.40-00 25 16.6	18.89	0.29	-0.24	-0.23	-0.21	0.22	11		DA4	
$14\ 20\ 58.38 + 01\ 07\ 28.9$	19.09	-0.22	-0.37	-0.36	-0.33	0.19	10		DA2.5	
14 21 20.19-00 46 26.1	17.59	0.42	-0.01	-0.32	0.09	0.26	50	287	DA4	
14 25 01.59-00 13 14.9	18.77	0.42	-0.09	-0.13	-0.20	0.19	44	277	DA3.5	
$14\ 25\ 39.74 + 01\ 09\ 26.9$	19.15	0.00	-0.27	-0.33	-0.40	0.16	56	189	DA2	
14 26 01.48+01 00 00.2	19.35	0.32	-0.33	-0.24	-0.22	0.16	35	166	DA3	
14 27 37.33-00 00 50.1	17.98	-0.38	-0.45	-0.36	-0.34	0.19	20	205	DA2	
14 28 46.41+00 45 26.4	18.54	0.42	-0.05	-0.06	-0.09	0.18	91	276	DA6	
14 31 54.58-00 12 31.4	18.40	0.45	-0.16	-0.17	-0.27	0.22	36	218	DA3	
14 31 59.73+00 02 16.1	17.86	0.34	-0.30	-0.22	-0.32	0.20	26	241	DA3	
14 34 25.45+00 53 06.4	20.08	-0.09	-0.23	-0.25	-0.30	0.21	9		DB4:	
14 37 24.41+00 56 07.6	20.02	0.25	-0.23	-0.27	-0.34	0.21	< 20		DA3:	
14 37 29.77+00 11 24.1	18.06	0.06	-0.34	-0.31	-0.33	0.23	20	302	DA2.5	
14 37 45.77+01 00 23.8	20.01	0.31	-0.31	-0.16	-0.44	0.22	24	159	DA2:	
14 37 51.82+00 52 54.9	17.54	0.13	-0.34	-0.27	-0.26	0.21	43	321	DA3	
14 38 01.04+01 07 38.3	17.60	-0.08	-0.39	-0.28	-0.36	0.21	40	311	DA2	
14 38 34.49-00 49 28.3	19.68	0.22	-0.28	-0.21	-0.08	0.22	25	250	DA2.5	
14 39 03.93-00 31 19.5	19.51	-0.13	-0.27	-0.23	-0.28	0.19	18		DB4	_
14 39 47.63-01 06 06.8	16.52	-0.36	-0.21	0.02	0.11	0.24	10		DA1+Me	5
14 40 15.58+00 24 41.5	18.61	0.50	-0.09	-0.11	-0.14	0.25	52	217	DA4	
14 40 28.76+00 39 39.6	19.46	-0.02	-0.35	-0.23	-0.24	0.23	29	226	DA2	
14 40 50.24-00 00 58.9	19.67	0.49	0.03	-0.08	-0.14	0.21	21	177	DA6	
14 40 50.84-01 07 12.8	19.91	0.10	-0.40	-0.27	0.02	0.26	20	180	DA2:	
14 41 08.43+01 10 20.0	16.87	-0.20	-0.43	-0.31	-0.28	0.21	12	200	DA1.5	
14 41 14.21+00 37 02.3	19.87	0.20	-0.24	-0.24	-0.30	0.23	34	206	DA2	
14 41 37.38-00 05 28.6	18.37	0.07	-0.33	-0.29	-0.16	0.19	40	232	DA2	
14 41 46.72-01 13 59.3	18.75	-0.29	-0.38	-0.32	-0.34	0.27	13	01.4	DA2	
14 42 08.86-00 27 36.9	17.88	-0.20	-0.40	-0.29	-0.25	0.19	42	214	DA2	-
14 42 58.48+00 10 31.5	18.34	0.05	0.07	0.80	0.73	0.21	19		DB3.5+M	5
14 43 12.69-00 06 58.0	18.66	0.45	-0.15	-0.20	-0.20	0.21	15		DA4	
14 43 51.29+01 04 20.0	18.07	0.11	-0.28	-0.26	-0.29	0.21	11	40	DA3	1 ~
14 44 33.80-00 59 58.9	16.22	0.37	-0.18	-0.20	-0.28	0.22	40	49	DA4	15
14 45 42.38-00 25 33.5	19.46	0.29	-0.24	-0.18	-0.29	0.18	32	188	DA3	
14 45 52.51+00 40 14.3	19.98	-0.19	-0.37	-0.32	-0.75	0.26	<20		DA1.5:	

Table 1. (continued)

Name SDSS J+	g	u-g	g-r	r-i	i-z	A_u	$\mu $ (mas/yr)	PA (deg)	Spec. Type	Note
14 46 59.29-00 39 45.9	19.97	0.03	-0.33	-0.30	-0.11	0.23	< 20		DA2	
$14\ 47\ 26.11{-}01\ 01\ 24.7$	19.78	0.38	-0.10	-0.14	-0.17	0.26	22	256	DA3.5:	
$14\ 48\ 28.21{-}01\ 05\ 25.4$	18.87	0.43	-0.18	-0.20	-0.26	0.24	16		DA3	
14 48 59.39+01 12 43.8	19.62	0.55	-0.20	-0.20	-0.02	0.24	30	169	DA3:	
14 49 25.91-00 49 18.0	19.88	0.28	-0.23	-0.24	-0.34	0.23	22	225	DA2:	
14 50 23.39-00 54 41.1	18.70	0.00	-0.21	-0.18	-0.26	0.23	37	250	DB4	
14 52 01.06+00 03 53.1	19.99	0.19	-0.32	-0.25	0.01	0.23	28	215	DA2	
14 52 47.31-00 46 34.2	18.81	0.47	-0.07	-0.12	-0.20	0.25	64	140	DA4	
14 53 00.99+00 55 57.1	19.21	0.48	0.06	0.61	0.49	0.27	54	213	DA3:+M	5
14 53 05.89-00 30 47.8	18.40	0.27	-0.27	-0.22	-0.22	0.30	41	234	DA2.5	
14 53 26.50+00 51 35.4	18.60	0.42	-0.03	-0.14	-0.11	0.28	43	235	DA5	
14 54 28.29+00 28 04.0	19.11	-0.27	-0.46	-0.31	-0.26	0.21	15		DA1.5	
14 55 35.49+01 02 46.5	18.95	0.43	-0.02	-0.04	-0.09	0.23	84	206	DA5-6	16
14 56 44.91+01 10 17.6	19.05	-0.03	-0.30	-0.16	-0.39	0.22	38	232	DB3.5	17
14 58 14.81+00 12 42.8	19.73	0.28	-0.20	-0.18	-0.45	0.26	13		DA3:	
14 59 29.25+00 33 20.3	18.97	-0.13	-0.40	-0.30	-0.18	0.27	20	223	DA2:	
14 59 47.05-00 39 54.6	18.40	-0.05	-0.28	-0.23	-0.20	0.32	65	187	DB3	18
15 00 03.86+00 24 19.9	18.80	0.04	-0.20	-0.15	-0.30	0.27	120	220	DB4	19
15 01 24.61+00 54 30.4	18.12	0.47	-0.06	-0.11	-0.16	0.24	43	223	DA5	
15 02 07.02-00 01 47.3	18.68	0.37	-0.14	-0.04	-0.22	0.32	45	228	DA3.5	
15 02 31.66+01 10 45.9	18.47	0.41	-0.04	0.44	0.54	0.25	215	203	DA3:+M	5,20
15 03 08.68-00 13 52.9	17.88	0.27	-0.25	-0.29	-0.20	0.30	27	285	DA3	- / -
15 03 15.53+00 58 23.3	20.34	0.40	-0.09	0.42	0.53	0.26	58	94	DA+M	
15 03 18.29-00 10 13.6	19.94	0.50	-0.21	-0.29	-0.06	0.30	25	144	DA:	
15 03 30.49-00 52 11.4	18.39	0.43	-0.15	-0.14	-0.14	0.31	26	247	DA3	
15 04 21.06-00 56 13.9	19.35	-0.16	-0.43	-0.33	-0.33	0.31	10		DA2	
15 05 56.90-00 03 38.9	20.14	0.49	-0.21	-0.20	-0.60	0.29	33	203	DA:	
15 06 48.12+00 27 16.4	19.11	0.26	0.57	0.75	0.49	0.31	40	273	DA+M	5
15 10 58.77+00 41 12.7	19.42	0.44	-0.05	0.38	0.62	0.23	69	178	DA3:+M	5
15 14 02.58+00 52 45.6	18.56	-0.39	-0.47	-0.37	-0.16	0.24	24	202	DA1	9
15 14 21.27+00 47 52.9	15.68	-0.20	-0.42	-0.32	-0.29	0.26	31	170	DA2	21
15 17 47.99-01 10 49.6	18.77	-0.19	-0.39	-0.20	-0.29	0.47	23	306	DA3	
15 18 33.21-00 56 41.6	19.12	0.44	0.06	-0.03	-0.01	0.31	65	291	DA6	
15 20 08.32+00 11 26.2	18.17	0.51	-0.06	-0.11	-0.30	0.33	<20	201	DA4	22
15 23 20.97+00 55 25.2	18.98	0.06	-0.20	-0.19	-0.06	0.25	30	160	DB4-5	22
15 27 17.26+00 24 13.3	19.64	0.56	-0.02	0.64	0.59	0.37	15	100	DA+M	5
15 27 28.27+00 22 01.7	19.15	-0.38	-0.48	-0.28	-0.28	0.37	13		DA1.5	9
15 28 39.42+01 13 00.1	16.43	-0.41	-0.52	-0.27	-0.27	0.24	17		DA1	23
15 29 33.26+00 20 31.2	18.21	0.49	-0.14	0.35	0.53	0.31	26	259	DA+Me	5
15 30 17.15+01 10 11.8	18.95	0.38	0.02	-0.04	-0.09	0.26	51	118	DA6	0
15 30 32.05+00 45 09.1	18.11	0.04	-0.10	-0.11	-0.19	0.26	64	237	DB:	
15 34 24.86+00 37 56.0	17.41	0.40	-0.02	0.03	-0.10	0.33	38	77	DA6	
15 34 37.70-00 47 19.5	17.49	-0.16	-0.39	-0.22	-0.28	0.61	$\frac{36}{25}$	135	DA2.5	
15 35 42.07+01 02 18.2	19.12	0.36	0.06	-0.08	-0.21	0.35	13	100	DA5	
15 39 31.54+00 01 18.4	17.88	-0.04	-0.36	-0.03 -0.27	-0.21 -0.36	$0.35 \\ 0.45$	26	234	DA3 DA2	
15 40 34.63-00 45 39.4	18.55	-0.04 0.56	-0.30 -0.04	-0.27 -0.08	-0.30 -0.15	0.43	36	$\frac{254}{259}$	DA2 $DA3.5$	
15 42 06.08+00 03 01.1	20.17	0.10	-0.04 -0.27	-0.08 -0.28	-0.13 -0.29	0.03 0.47	14	203	DA3.5 DA3:	
15 42 44.07-00 04 58.7	17.95	0.10 0.12	-0.27 -0.31		-0.29 -0.29	0.47	10		DA3. DA2.5	
15 43 13.53+00 29 57.6		-0.12 -0.09	-0.31 -0.23	-0.26 -0.20	-0.29 -0.11	0.48 0.52			DB3-4	
	19.07						5 47	200	DB3-4 DA3	
15 44 43.55+00 38 17.9	19.14	0.03	-0.28	-0.22	-0.11	0.49	47	208	DA3 DA4	
15 46 20.51+01 08 48.7	19.06	0.36	-0.18	-0.26	0.04	0.50	12			
15 46 35.06-00 53 11.9	20.18	0.38	-0.22	-0.28	0.05	0.53	<20		DA4.5	

Table 1. (continued)

Name SDSS J+	g	u-g	g-r	r-i	i-z	A_u	μ (mas/yr)	PA (deg)	Spec. Type	Note
15 46 39.84+00 59 16.8	18.74	0.38	-0.24	-0.17	-0.18	0.50	26	245	DA4	
$15\ 46\ 47.29{-00}\ 50\ 03.6$	18.04	0.12	-0.30	-0.20	-0.25	0.54	25	263	DA3	
$15\ 47\ 03.51 + 00\ 28\ 19.3$	19.90	0.29	-0.25	-0.24	0.04	0.48	7		DA3	
$15\ 48\ 32.76{-00}\ 17\ 18.0$	18.18	0.40	-0.03	-0.10	-0.09	0.48	55	273	DA5	
$15\ 49\ 32.35 + 00\ 22\ 45.2$	19.56	0.31	-0.23	-0.19	-0.28	0.39	12		DA3.5	
$15\ 49\ 38.64{-00}\ 13\ 18.3$	20.23	0.16	-0.09	-0.25	-0.19	0.43	22	238	DB:	
$15\ 49\ 49.93 + 01\ 08\ 47.5$	19.85	0.41	-0.04	-0.16	-0.03	0.49	29	250	DA4.5	
$15\ 50\ 43.25{-}01\ 06\ 36.3$	19.40	-0.01	-0.26	-0.18	-0.12	0.68	18		DA3	
$15\ 50\ 58.48{+}01\ 07\ 10.2$	20.09	-0.40	-0.44	-0.28	0.12	0.42	15		DA:	
$15\ 52\ 22.54{+}00\ 37\ 24.4$	18.24	-0.15	-0.37	-0.31	-0.26	0.44	18		DA2	
$15\ 52\ 38.22+00\ 39\ 10.4$	18.44	0.10	-0.19	-0.23	-0.26	0.46	49	137	DA3	
$15\ 52\ 43.05{-}00\ 05\ 24.5$	18.78	0.07	-0.28	-0.22	-0.16	0.48	41	217	DA3.5	
$15\ 53\ 16.22+00\ 31\ 53.4$	19.75	0.23	-0.20	-0.20	-0.25	0.45	9		DA5:	
$15\ 53\ 40.36 + 01\ 13\ 35.3$	19.35	0.08	-0.18	-0.16	-0.21	0.51	12		DB4	
$15\ 54\ 06.58{+}00\ 34\ 53.3$	19.32	0.43	-0.01	-0.15	-0.23	0.52	19		DA5	
$15\ 54\ 12.85 + 01\ 11\ 19.8$	18.54	0.25	-0.25	-0.20	-0.25	0.54	28	264	DA3	
$15\ 54\ 49.44+00\ 11\ 51.2$	19.43	0.26	-0.22	-0.27	-0.42	0.55	39	193	DA3	
$15\ 56\ 02.62{-}00\ 07\ 21.7$	19.45	0.08	-0.28	-0.18	-0.25	0.65	41	274	DA2.5	
$16\ 00\ 08.07{-}00\ 08\ 40.4$	18.66	0.49	0.05	-0.04	-0.09	0.63	41	311	DA5	
$16\ 01\ 34.75 + 00\ 30\ 46.9$	19.95	0.37	-0.17	-0.24	-0.45	0.74	49	275	DA4	
$16\ 04\ 37.77 + 00\ 52\ 06.7$	19.65	0.09	-0.20	-0.15	-0.23	0.84	21	148	DB2:	
$16\ 05\ 54.53{-}00\ 28\ 11.2$	16.66	0.42	-0.04	-0.07	-0.15	0.78	144	320	DA5	
$16\ 06\ 16.54{-00}\ 35\ 52.0$	18.59	0.46	-0.09	-0.17	-0.14	0.69	8		DA4	
$16\ 09\ 16.74{-00}\ 07\ 01.0$	18.20	0.57	0.04	-0.08	-0.09	0.61	36	159	DA5	
16 09 18.48-00 31 18.8	18.81	0.55	0.22	0.08	0.01	0.69	123	218	DA7	
$16\ 10\ 07.98+00\ 51\ 37.4$	19.10	0.01	-0.35	-0.26	-0.07	0.71	20	321	DA3	
$16\ 11\ 10.01 + 00\ 05\ 32.5$	18.87	0.48	0.12	0.06	-0.04	0.67	10		DA7:	
16 11 31.70+00 10 18.1	19.08	0.15	0.62	0.57	0.35	0.68	36	221	DA+M	
$16\ 11\ 45.89{+}01\ 03\ 27.8$	18.65	0.57	0.12	0.61	0.70	0.59	34	165	DA5+M	5
$16\ 12\ 25.69{+}00\ 10\ 27.8$	20.26	0.30	-0.15	-0.22	-0.58	0.68	10		DA4:	
16 14 41.51+01 05 57.0	19.13	0.49	-0.24	-0.23	0.05	0.54	33	300	DA4.5	
$16\ 14\ 52.94{+}00\ 16\ 32.4$	19.01	0.47	0.10	0.03	-0.16	0.57	84	272	DA6.5:	
$16\ 18\ 37.25{-00}\ 23\ 02.7$	19.26	0.42	-0.12	-0.20	-0.08	0.50	32	278	DA5	
16 19 31.75+00 57 31.0	18.65	0.51	0.04	0.21	0.43	0.41	49	258	DA+M	
$16\ 30\ 47.89{-00}\ 03\ 29.8$	19.73	0.13	-0.31	-0.20	-0.09	0.50	26	243	DA3	
16 32 00.33-00 19 28.3	18.41	-0.40	-0.42	-0.32	-0.33	0.48	19		DAO1	
$16\ 32\ 09.00+00\ 26\ 29.9$	19.89	0.55	0.46	0.33	0.35	0.48	7		DA+K:	
16 33 19.20-00 06 09.0	20.07	-0.12	-0.34	-0.31	-0.08	0.48	< 20		DA1.5	
$16\ 36\ 27.68{-00}\ 29\ 50.3$	18.65	0.23	-0.23	-0.22	-0.33	0.65	14		DA3	
16 38 00.36+00 47 17.8	18.84	-0.34	-0.43	-0.33	-0.14	0.45	5		DA1	
$16\ 38\ 07.33{-}00\ 08\ 37.7$	19.88	0.08	-0.19	-0.23	-0.03	0.56	12		DB4	

 $^{^{1}\}mathrm{HS}0944{+}0127$

²WD0948+013, PG0948+0118 ³WD0955-008, PG0955-0049 ⁴WD1000-001, PG1000-0009

⁵WD+M composite spectrum studied by Raymond et al. (2003).

⁶WD1236-004

⁷Blended image, proper motion not well determined. ⁸Resolved pair, 4" separation (probably a third star).

⁹HE1258+0123

¹⁰HE1314+0018, PG1314+0018

¹¹HS1329+0121 12WD1336+001 13HS1352+0123 14WD1352+004, PG1352+0026

 $^{^{15}\}mathrm{HE}1441{-}0047$

 $^{^{16}\}mathrm{WD1453}{+}012$

 $^{^{17}}WD1454+013$

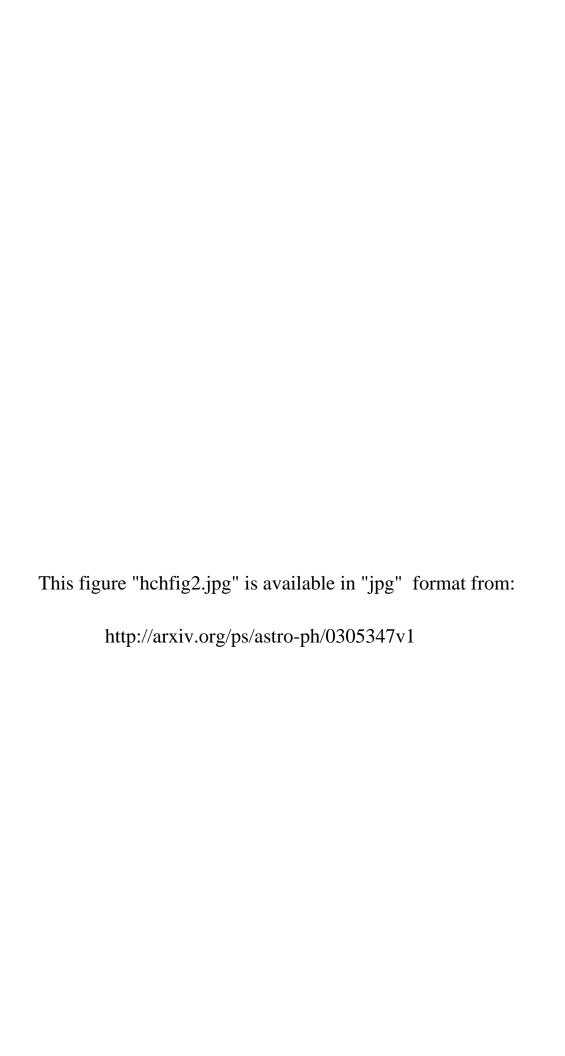


Table 2. Unusual White Dwarfs

Name SDSS J+	g	u-g	g-r	r-i	i-z	A_u	$\mu \pmod{\operatorname{yr}}$	PA (deg)	Spec. Type	Note
Other hot DO and DB st	tars (Fig.	4):								
01 56 29.60+13 17 44.8	18.10	-0.15	-0.29	-0.22	-0.26	0.29	7		DB2	
03 42 27.63-07 22 13.3	17.64	-0.36	-0.48	-0.36	-0.33	0.27	22	112	DO	
Magnetic DAH stars (Fig										
03 04 07.40-00 25 41.8	17.75	0.32	-0.18	-0.19	-0.25	0.53	24	251	DAH	1
03 31 45.69+00 45 17.0	17.21	0.06	-0.25	-0.24	-0.28	0.52	33	95	DAH	1,2
03 45 11.11+00 34 44.3	18.63	0.41	0.13	-0.02	-0.01	0.77	52	235	DAH	1
08 58 30.85+41 26 35.1	17.08	0.51	0.20	0.10	-0.11	0.12	392	194	DAH	3
10 18 05.04+01 11 23.5	16.28	0.24	-0.15	-0.12	-0.18	0.22	58	201	DAH	4
11 38 39.51-01 49 03.0	17.58	0.35	-0.14	-0.21	-0.22	0.13	46	250	DAH	5
11 54 18.14+01 17 11.4	17.75	-0.28	-0.41	-0.30	-0.35	0.09	84	234	DAH	
12 16 35.37-00 26 56.2	19.60	0.27	-0.27	-0.22	-0.03	0.10	22	204	DAH	1
$13\ 33\ 40.34{+}64\ 06\ 27.4$	17.88	0.28	-0.22	-0.15	-0.31	0.12	64	118	DAH	
13 40 43.10+65 43 49.2	18.42	0.32	-0.32	-0.21	-0.28	0.11	25	273	DAH	
$15\ 42\ 13.48{+}03\ 48\ 00.4$	19.11	0.44	0.00	-0.12	-0.21	0.32	42	289	DAH	
17 20 45.37+56 12 14.9	20.10	-0.11	-0.37	-0.25	-0.58	0.13	19		DAH	1
$17\ 23\ 29.14 + 54\ 07\ 55.8$	18.78	0.32	-0.07	-0.16	-0.26	0.29	77	150	DAH	1
$20\ 46\ 26.15{-}07\ 10\ 37.0$	17.99	0.34	0.09	-0.06	-0.06	0.40	69	119	DAH	
$22\ 47\ 41.46{+}14\ 56\ 38.8$	17.41	-0.04	-0.22	-0.33	-0.27	0.47	77	168	DAH	
23 22 48.22+00 39 00.9	19.14	-0.20	-0.28	-0.18	-0.25	0.21	21	54	DAH	1
Magnetic DBH stars (Fig	g. 6):									
$00\ 17\ 42.44 + 00\ 41\ 37.4$	16.93	-0.06	-0.25	-0.24	-0.22	0.14	45	218	DBH	
$01\ 42\ 45.37{+}13\ 15\ 46.4$	17.70	-0.08	-0.30	-0.21	-0.24	0.26	20	156	DBH	
$03\ 33\ 20.37{+}00\ 07\ 20.7$	16.53	0.52	0.08	0.07	-0.10	0.47	93	97	DB:HP	1,6
DQ stars with C ₂ Swan		and/or C	III lines (F	igs. 7–8):						
00 25 31.50-11 08 00.8	18.00	0.16	-0.01	-0.13	-0.19	0.17	135	125	DQ	
$01\ 54\ 41.74 + 14\ 03\ 08.0$	17.88	0.52	0.23	0.08	-0.07	0.38	276	143	DQ	7
$03\ 20\ 54.11 - 07\ 16\ 25.4$	19.71	0.24	0.46	0.08	0.00	0.27	126	96	DQ	
03 32 18.22-00 37 22.1	18.28	0.35	-0.03	-0.11	-0.19	0.63	177	179	DQ	
08 08 43.15+46 40 28.7	20.39	0.37	1.00	0.26	0.07	0.29	100	94	DQ	
09 01 57.92+57 51 35.9	18.53	-0.14	-0.32	-0.22	-0.34	0.15	63	84	DQ CI	
09 19 22.18+02 36 05.0	18.96	0.00	-0.23	-0.18	-0.32	0.21	121	128	DQ CI	
$09\ 35\ 37.00+00\ 24\ 22.0$	20.14	0.15	0.96	0.51	0.00	0.25	65	48	$\overline{\mathrm{DQ}}$	
09 40 04.64+02 10 22.6	17.27	0.39	0.14	-0.05	-0.08	0.26	87	239	$\overline{\mathrm{DQ}}$	
11 13 41.33+01 46 41.7	19.24	-0.58	0.74	0.17	0.19	0.17	412	207	DQH	
11 46 35.23+00 12 33.6	14.88	-0.52	-0.55	-0.41	-0.36	0.15	17		DQZ01	8,9
11 48 51.68-01 26 12.8	17.38	0.00	-0.07	-0.13	-0.25	0.10	151	209	DQ CI	_
11 53 05.55+00 56 46.2	18.89	-0.49	-0.48	-0.27	-0.31	0.10	147	250	DQ CII	8
13 33 59.86+00 16 54.8	19.41	-0.36	1.09	0.26	-0.09	0.14	386	301	DQH	8,10
13 37 10.19-00 26 43.7	18.70	-0.48	-0.46	-0.35	-0.30	0.14	7		DQ CII	8
13 56 28.25-00 09 41.2	18.60	0.35	0.32	0.05	-0.06	0.21	206	225	DQ	8,11
14 27 28.30+61 10 26.4	17.14	0.58	0.23	0.06	-0.04	0.07	271	272	DQ	12
14 48 08.07-00 47 55.9	18.41	0.42	0.14	0.01	-0.13	0.24	42	273	DQ	8
15 54 13.53+03 36 34.5	18.89	0.55	0.23	0.03	-0.08	0.86	141	139	DQ DOAD CI	10
17 28 56.22+55 58 22.8	15.98	-0.14	-0.34	-0.24	-0.26	0.19	256	334	DQAB CI	13
20 53 16.34-07 02 04.3	19.22	0.11	0.47	0.13	-0.12	0.42	111	169	DQ	1.4
22 32 24.00-07 44 34.3	18.38	0.03	0.59	0.13	-0.09	0.27	277	243	DQ	14
23 10 30.26-00 57 45.8	19.12	0.22	0.12 Fina 0.11	-0.01	-0.09	0.19	30	292	DQ	
DZ stars with metallic al	-	,	_		0.00	0.05	100	90	DAZ:	1 5
01 35 04.11+13 02 40.5	19.32	1.50	0.29	0.05	-0.06	0.25	103	30	DAZ:	15
01 57 48.15+00 33 15.2	19.59 17.56	2.00	0.40	0.03	-0.13	0.14	37	153	DZH:	15 15
02 01 32.24-00 39 32.0	17.56	0.21	-0.14	-0.16	-0.23	0.14	90	189	DZ	15

Table 2. (continued)

Name SDSS J+	g	u-g	g-r	r-i	i-z	A_u	μ (mas/yr)	PA (deg)	Spec. Type	Note
09 37 19.14+52 28 02.3	19.44	1.36	0.26	-0.10	-0.01	0.07	70	271	DZ	15,16
$09\ 39\ 42.30+55\ 50\ 48.7$	16.75	0.30	-0.08	-0.15	-0.20	0.11	99	274	DZA	15
$09\ 44\ 31.28{-}00\ 39\ 33.7$	17.75	0.09	-0.24	-0.19	-0.20	0.32	36	153	DBZ	8
$09\ 56\ 45.15 + 59\ 12\ 40.6$	18.37	0.57	-0.02	-0.16	-0.21	0.05	124	249	DZA	15,16
$10\ 38\ 09.19{-00}\ 36\ 22.5$	16.98	0.75	0.03	-0.14	-0.23	0.30	98	277	DZ	15,16
$11\ 22\ 58.34{+}50\ 41\ 46.8$	19.27	0.39	-0.11	-0.19	-0.23	0.10	45	254	DZ	15
$12\ 27\ 33.46{+}63\ 30\ 29.5$	18.22	0.63	0.06	-0.12	-0.15	0.10	144	265	DZ	15,16
$13\ 30\ 01.13{+}64\ 35\ 23.8$	21.57		0.64	0.87	0.17	0.12	193	270	DZ :	16
$13\ 41\ 44.10{-}01\ 12\ 38.4$	19.70	0.37	0.01	-0.14	-0.25	0.14	22	197	DZ	8
$14\ 14\ 26.55{-}01\ 13\ 54.7$	17.85	0.23	-0.05	-0.09	-0.20	0.27	116	268	DZ	8
$14\ 25\ 16.43{-00}\ 50\ 48.9$	18.04	0.46	0.08	-0.01	-0.10	0.25	70	256	DZ	8
$16\ 00\ 12.54{-00}\ 09\ 05.3$	19.65		0.47	0.09	0.18	0.63	7		DZ :	8
DC stars without signific	ant featur	res (Fig. 9	9):							
$11\ 22\ 28.69{-00}\ 08\ 58.6$	19.51	0.13	-0.10	-0.20	-0.24	0.17	44	136	DC	8
$11\ 27\ 53.50{-}00\ 33\ 24.5$	19.82	-0.02	-0.16	-0.23	-0.24	0.14	60	244	DC:	8
$13\ 37\ 39.41 + 00\ 01\ 42.7$	19.57	1.26	0.44	-0.39	-0.50	0.13	186	184	DC+cia	8
14 09 16.34-00 00 11.3	18.79	0.35	0.14	-0.05	-0.10	0.18	41	253	DC	8
$14\ 56\ 02.80{-}01\ 09\ 52.6$	18.62	0.42	0.09	-0.02	-0.17	0.28	45	277	DC	8
15 05 16.97+00 16 59.6	19.22	0.08	-0.13	-0.16	-0.31	0.31	26	151	DC:	8
$15\ 48\ 50.76{+}00\ 18\ 52.2$	19.07	0.24	0.00	-0.09	-0.08	0.39	58	163	DC5	8
$16\ 10\ 44.46{+}00\ 46\ 50.5$	18.10	0.19	-0.02	-0.12	-0.13	0.72	80	260	DC:	8
$16\ 18\ 37.41{+}00\ 25\ 24.9$	19.87	0.16	0.62	0.42	0.31	0.44	2		DC:+sdM	8
16 54 01.30+62 53 55.0	18.40	1.30	0.53	-0.20	-0.28	0.25	566	286	DC+cia	17

 $^{^{1}{\}rm Discussed}$ by Gänsicke et al. (2002). $^{2}{\rm WD0329{+}005{=}KUV03292{+}0035}$

 $^{^{3}{}m LP210-13}$

 $^{^{4}}$ WD1015+014

 $^{^{5}}$ WD1136-015=LPQS1136-0132

⁶HE0330-0002

 $^{^{7}\}mathrm{LP468-295}$

⁸Star is in the 41-plate region of Tables 1 and 3.

 $^{^{9}} WD1144 + 004$

 $^{^{10}{}m LP618-6}$

¹¹LP619-3

¹²WD1426+613=GR362 ¹³WD1727+560=G227-5=GR441 ¹⁴LP700-32 ¹⁵Spectrum shows MgI (Fig. 10). ¹⁶Spectrum shows NaI (Fig. 10).

 $^{^{17}\}mathrm{LHS}~3250$

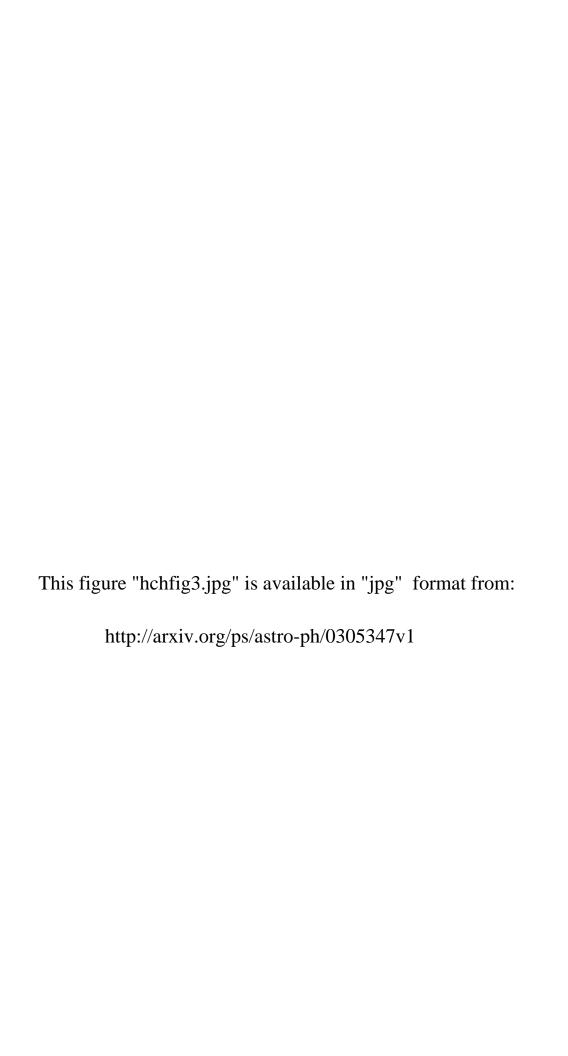


Table 3. Hot Subdwarfs

=	Name SDSS J+	g	u-g	g-r	r-i	i-z	A_u	$\mu $ (mas/yr)	PA (deg)	Spec. Type	Note
-	09 40 44.08+00 47 59.7	18.99	-0.17	-0.19	-0.11	-0.02	0.51	12		sdB-He	
	10 00 19.99-00 34 13.4	17.52	-0.44	-0.52	-0.39	-0.33	0.22	16		sdO	
	11 14 38.57-00 40 24.3	18.19	-0.48	-0.45	-0.37	-0.23	0.26	13		sdO	
	11 33 12.12+01 08 24.8	17.75	0.50	-0.29	-0.26	-0.17	0.15	1		sdB	
	11 38 40.69-00 35 31.8	14.18	-0.25	-0.48	-0.44	-0.27	0.09	30	194	$\operatorname{sdB-He}$	1
	12 43 46.38+00 25 35.1	18.61	0.23	0.03	0.02	0.04	0.10	14		sdB :-He	
	12 47 06.79-00 39 25.8	16.18	-0.40	-0.52	-0.32	-0.32	0.17	6		sdB	2
	12 54 10.86-01 04 08.4	17.43	0.05	-0.42	-0.29	-0.26	0.10	16		$\operatorname{sdB-He}$	
	12 59 41.88-00 39 28.8	16.81	0.01	-0.12	-0.09	-0.07	0.11	13		sdO	
	13 00 25.53+00 45 30.1	15.67	-0.19	-0.15	-0.09	-0.10	0.13	23	182	sdO	3
	13 00 59.20+00 57 11.7	16.28	-0.34	-0.38	-0.23	-0.16	0.13	16		sdO	4
	13 17 45.80+01 04 50.5	16.61	-0.05	-0.47	-0.34	-0.20	0.17	10		$\operatorname{sdB-He}$	5
	13 31 21.45-00 17 49.5	19.71	-0.18	-0.36	-0.19	-0.05	0.13	13		sdB:	
	13 35 48.55-00 54 23.0	19.74	0.26	-0.39	-0.26	-0.42	0.15	7		sdB	
	13 36 11.02-01 11 56.0	18.34	-0.38	-0.48	-0.32	-0.35	0.14	12		$\operatorname{sdB-He}$	
	13 45 45.23-00 06 41.7	17.54	-0.16	-0.24	-0.14	-0.15	0.14	12		$\operatorname{sdB-He}$	
	13 46 35.68-00 18 04.7	18.81	0.10	-0.33	-0.34	-0.19	0.14	5		$\operatorname{sdB-He}$	
	13 50 25.82-01 10 35.5	19.47	-0.31	-0.49	-0.32	-0.28	0.24	4		sdO	
	13 57 07.34+01 04 54.6	17.25	0.00	-0.10	-0.10	0.03	0.18	12		$\operatorname{sdB-He}$	
	14 15 56.68-00 58 15.0	18.39	-0.36	-0.37	-0.24	-0.21	0.23	18		$\operatorname{sdB-He}$	
	14 31 53.06-00 28 24.4	17.82	-0.32	-0.50	-0.68	0.05	0.24	14		sdO	
	14 38 12.57+00 16 41.5	19.11	-0.21	-0.41	-0.31	-0.20	0.24	5		sdB	
	14 39 17.64+01 02 51.1	16.42	0.01	-0.36	-0.28	-0.28	0.21	10		$\operatorname{sdB-He}$	
	14 45 14.93+00 02 48.9	17.34	-0.02	-0.15	-0.04	-0.11	0.22	13		$\operatorname{sdB-He}$	
	14 48 20.30-01 08 33.7	18.74	0.12	-0.09	-0.06	-0.08	0.25	10		sdB	
	15 12 31.29+00 53 17.7	18.00	-0.30	-0.47	-0.33	-0.34	0.24	11		sdO	
	15 13 06.73+01 14 39.2	17.06	-0.09	-0.42	-0.33	-0.26	0.25	15		sdB	
	15 21 51.97-00 23 59.7	18.04	0.05	-0.37	-0.32	-0.22	0.32	16		sdB	
	15 26 07.88+00 16 40.8	16.60	-0.46	-0.46	-0.39	-0.32	0.33	15		sdO	
	15 27 08.31+00 33 08.4	18.58	-0.34	-0.46	-0.34	-0.17	0.39	18		$\operatorname{sdB-He}$	
	15 29 05.62+00 21 37.5	18.15	-0.23	-0.46	-0.33	-0.30	0.32	14		$\operatorname{sdB-He}$	
	15 42 38.42-00 37 59.0	19.06	-0.09	-0.28	-0.29	-0.19	0.57	14		$\operatorname{sdB-He}$	
	15 43 38.69+00 12 02.1	16.76	-0.03	-0.28	-0.12	-0.13	0.45	7		sdB	
	15 48 09.97-00 49 31.4	16.43	-0.09	-0.20	-0.08	-0.02	0.51	8		sdB	
	15 56 28.35+01 13 35.0	16.03	-0.12	-0.37	-0.31	-0.19	0.47	9		sdB	
	16 02 41.13-00 12 07.1	17.49	-0.15	-0.32	-0.22	-0.21	0.68	16		$\operatorname{sdB-He}$	
	16 04 01.09+00 08 26.1	18.48	-0.11	-0.35	-0.20	-0.32	0.88	15		sdO	
	16 08 20.50-00 34 10.5	18.72	-0.06	-0.31	-0.20	-0.23	0.85	13		sdO:	
	16 09 18.67+00 22 21.1	17.80	0.28	0.14	0.07	0.02	0.60	19		$\operatorname{sdB-He}$	
	16 12 30.87+00 42 37.1	18.38	-0.30	-0.40	-0.29	-0.24	0.66	12		sdO	
	16 13 28.22+00 47 03.2	17.76	0.13	-0.30	-0.24	-0.21	0.59	12		sdB	
	16 14 31.33+00 40 04.5	18.72	-0.37	-0.44	-0.37	-0.04	0.52	8		sdO	
	16 16 27.11-00 29 33.0	17.72	-0.31	-0.41	-0.26	-0.24	0.65	13		sdO	
	16 16 31.29-00 38 53.3	16.72	-0.14	-0.23	-0.10	-0.11	0.59	9		sdO:	
	16 16 43.70-00 24 01.5	18.52	-0.24	-0.50	-0.19	-0.33	0.61	10		$\operatorname{sdB-He}$	
	16 19 15.35-00 56 16.0	19.12	-0.22	-0.34	-0.29	-0.27	0.54	11		sdO	
	16 19 47.78-00 37 36.7	17.96	0.08	-0.10	-0.15	-0.15	0.51	10		sdB:-He	
	16 22 50.09+00 26 32.0	16.75	-0.11	-0.37	-0.27	-0.28	0.40	14		sdB-He	
	16 33 06.59+00 32 16.3	16.90	-0.17	-0.37	-0.30	-0.26	0.51	6		sdB	
	16 34 46.48-00 53 45.6	16.92	0.08	-0.19	-0.12	-0.05	0.61	14		sdB-He	
	16 35 09.13+00 02 35.0	17.92	-0.06	-0.40	-0.27	-0.26	0.50	23	207	sdB	
	$16\ 35\ 32.56{+00}\ 29\ 54.4$	19.41	-0.25	-0.41	-0.26	-0.30	0.55	21	193	$\operatorname{sdB-He}$	

Table 3. (continued)

Name SDSS J+	g	u-g	g-r	r-i	i-z	A_u	μ (mas/yr)	PA (deg)	Spec. Type	Note
16 37 02.79-01 13 51.8 16 38 00.17+01 02 59.7 16 38 15.97-00 19 19.2	17.12 17.08 17.89	-0.31 0.34 0.19	-0.33 -0.26 -0.27	-0.24 -0.24 -0.23	-0.31 -0.17 -0.28	$0.75 \\ 0.41 \\ 0.63$	13 20 10	183	sdO sdB-He sdB-He	
$16\ 38\ 38.24{-00}\ 54\ 17.5$	19.65	-0.23	-0.33	-0.29	-0.06	0.69	22	190	sdO:	

 $^{{}^{1}}PG1136-0018$ ${}^{2}PG1244-0023 = TON 126$

³PG1257+0101

⁴PG1258+0113 = HE1258+0123 ⁵PG1315+0120

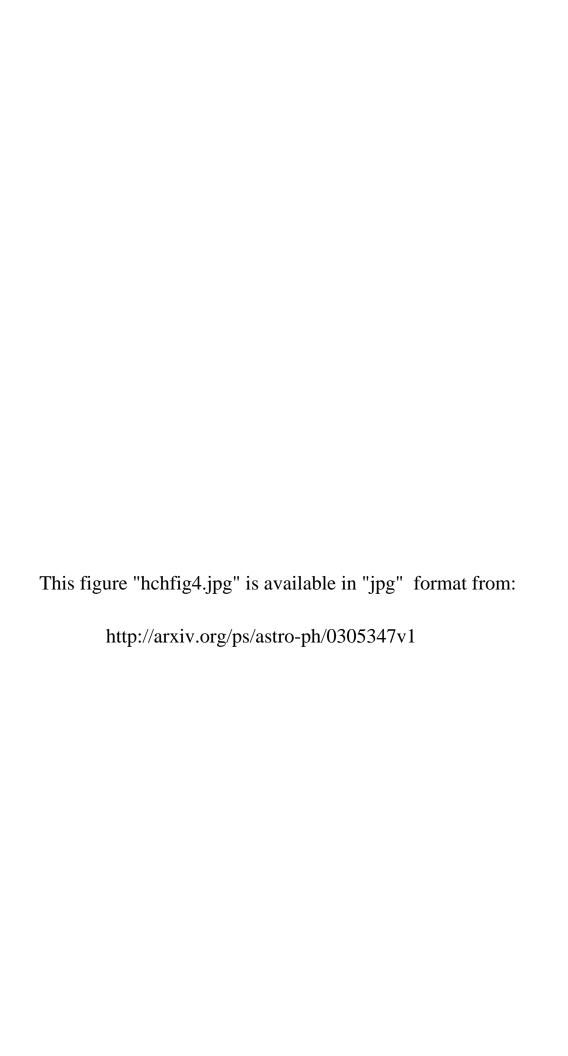


Table 4. Density of Blue Stars with $15 < g < 20\,$

	Observed Number		_	bserved ity (deg^{-2})	Adjusted Density (\deg^{-2})			
	Hot	Medium	Hot	Medium	Hot	Medium	Both	
DA	52	73	0.3	0.4	0.4	1.2	1.6	
DB	21	1	0.1	0.0	0.2	0.0	0.2	
Other	3	0	0.0	0.0	0.0	0.0	0.0	
All WDs	76	74	0.4	0.4	0.6	1.2	1.8	
sdB/sdO	42	6	0.2	0.0	0.3	0.1	0.4	
All Stars	118	118 80		0.4	0.9	1.3	2.2	

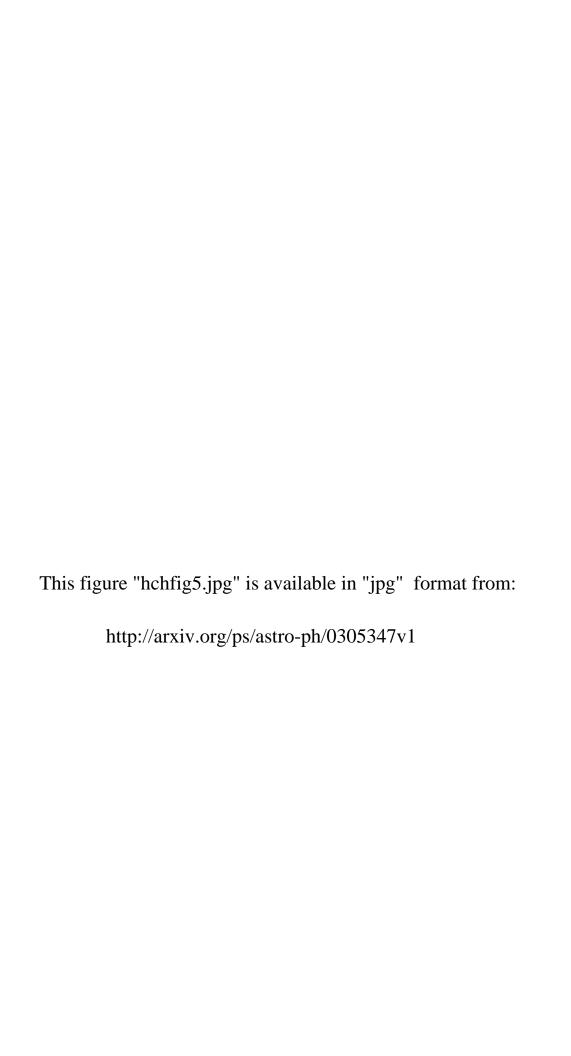


Table 5. Density of Hot WDs and sdB/sdO Stars

g	Observed Number			erved (\deg^{-2})	Adjusted Density (deg^{-2})		
	WDs	SDs	WDs	SDs	WDs	SDs	
15–16	5	0	0.03	0.00	0.03	0.00	
16 - 17	4	12	0.02	0.06	0.02	0.07	
17 - 18	13	10	0.07	0.05	0.08	0.06	
18 - 19	25	13	0.13	0.07	0.15	0.08	
19 - 20	29	7	0.15	0.04	0.33	0.08	
All	76	42	0.4	0.2	0.6	0.3	

